iScience

CellPress

Article

CdpR Inhibits CRISPR-Cas Adaptive Immunity to Lower Anti-viral Defense while Avoiding Self-Reactivity

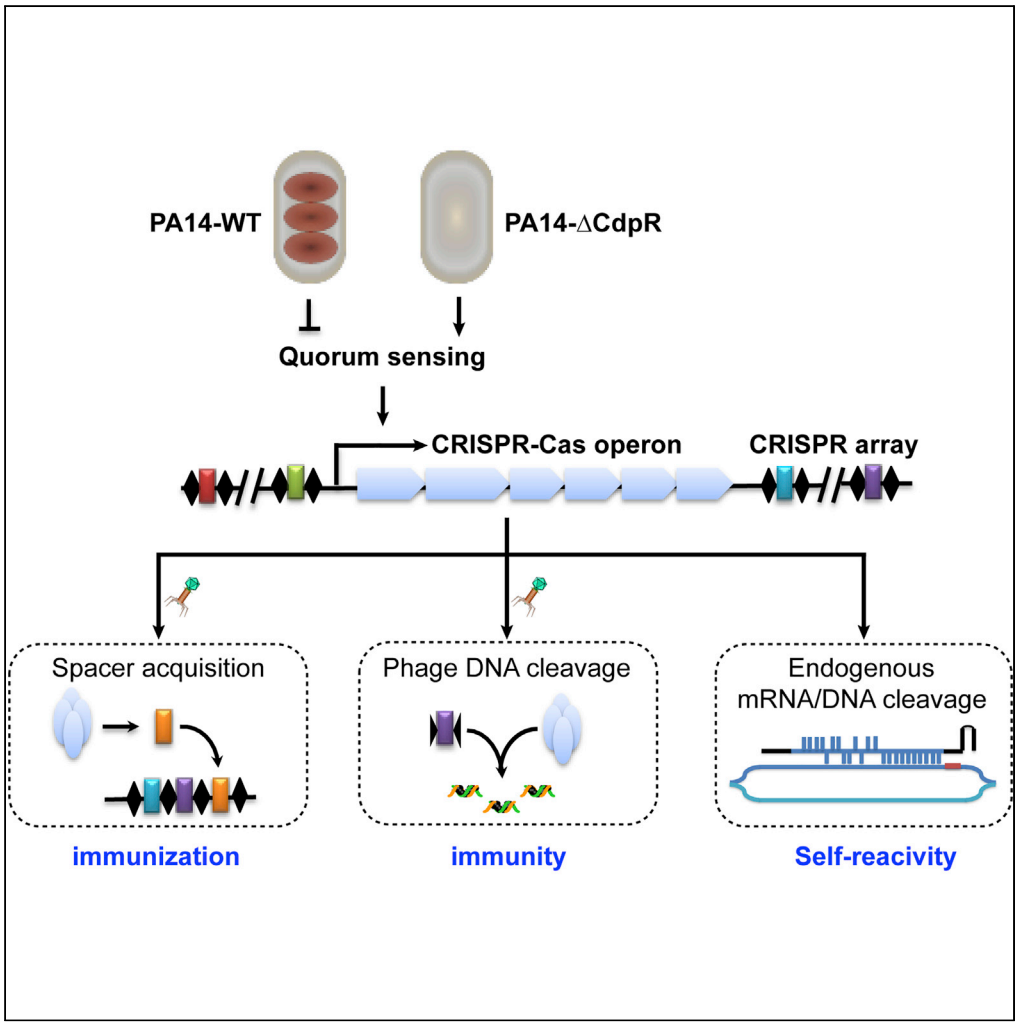

Ping Lin, Qinqin Pu, Guanwang Shen, ..., Haihua Liang, Jianxin Jiang, Min Wu

lianghh@nwu.edu.cn (H.L.)
hellojjx@126.com (J.J.)
min.wu@med.und.edu (M.W.)

HIGHLIGHTS

Both CRISPR-Cas immunization and immunity are suppressed by CdpR

CdpR prevents bacterial defense to phage infection via CRISPR-Cas systems

CdpR represses QS to modify CRISPR-Cas functionality in a Vfr-dependent manner

CdpR blocks Vfr binding to *cis*-response elements in the promoter of *cas* operon

Lin et al., iScience *13*, 55–68
March 29, 2019
https://doi.org/10.1016/j.isci.2019.02.005

iScience

CellPress

Article

CdpR Inhibits CRISPR-Cas Adaptive Immunity to Lower Anti-viral Defense while Avoiding Self-Reactivity

Ping Lin,[1,2,6] Qinqin Pu,[2,6] Guanwang Shen,[3] Rongpeng Li,[2,4] Kai Guo,[2] Chuanmin Zhou,[2] Haihua Liang,[5,*] Jianxin Jiang,[1,*] and Min Wu[2,7,*]

SUMMARY

CRISPR-Cas systems as adaptive immunity in bacteria and archaea battle against bacteriophages. However, little is known how CRISPR-Cas systems are precisely regulated to effectively eliminate intruders while not inducing self-reactivity. Here, we identify intrinsic negative modulator of CRISPR-Cas that influences interference and adaptation functions. LasI/RhlI-derived autoinducers activate *cas* operon by enhancing the binding of virulence factor regulator (Vfr) *cis*-response elements to *cas1* promoter, whereas CdpR represses this intracellular signaling and blocks transcription of *cas* operon. Importantly, inhibition of Vfr reduces *cas1* expression and impairs immunization and immune memory mediated by CRISPR-Cas, leading to more severe phage infection but lower self-targeting activities. In addition, CdpR-mediated LasI/RhlI/Vfr intracellular signaling represses cleavage of bacterial endogenous sequences by impeding Cas3 RNA cleavage activity. Thus, CdpR renders important inhibitory effects on CRISPR-Cas systems to avoid possible self-reactivity but potentially heightening infection risk. Our study provides insight into fine regulation of CRISPR-Cas systems for maintaining homeostasis.

INTRODUCTION

Bacteria have evolved multiple defense strategies to resist bacteriophage infection (Koonin et al., 2017; Labrie et al., 2010; Mohanraju et al., 2016). The clustered regularly interspaced short palindromic repeats (CRISPR) and their CRISPR-associated (Cas) systems are the first identified and only adaptive immunity against the foreign invaders and mobile genetic elements (MGEs) via *cas* genes and CRISPR arrays (Barrangou et al., 2007; Marraffini, 2015; Marraffini and Sontheimer, 2008). The CRISPR arrays consist of DNA remnants from foreign invaders (mostly from phages) to generate CRISPR RNAs (crRNAs) that target nucleic acids in a sequence-specific manner (Garneau et al., 2010). Cas proteins play a critical role in mediating the acquisition of foreign sequences into a CRISPR array (adaptation or immunization) (Heler et al., 2015; McGinn and Marraffini, 2016), facilitating the maturation of crRNAs (Deltcheva et al., 2011), and counteracting invasion of MGEs, DNA (Fonfara et al., 2016), or RNA (East-Seletsky et al., 2016). Both immunization and immunity processes require activation of CRISPR-Cas systems. Currently, two distinct classes of CRISPR-Cas systems have been identified, which are further divided into a series of subtypes based on their distinct Cas effector machineries with substantial differences in targeting mechanisms (Lewis and Ke, 2017; Makarova et al., 2015). New CRISPR-Cas systems have been continuously discovered (Burstein et al., 2017; Smargon et al., 2017). The current understanding of the adaptive immunity is that CRISPR-Cas systems enable bacteria to distinguish nucleic acids between self and foreign sources, relying on the recognition of spacers and protein-mediated protospacer adjacent motif (PAM) to avoid autoimmunity (Hayes et al., 2016; Rollins et al., 2015; Westra et al., 2012, 2013). CRISPR-Cas systems are important for adaptive immunity for bacteria or archaea to survive in adverse environments by combatting numerous phages; however, many intriguing questions remain to be answered (Ledford, 2017). For instance, how do bacteria regulate CRISPR-Cas systems to shape and balance host defense and homeostasis?

To effectively defend against phages or MGEs, bacterial CRISPR-Cas systems rapidly evolved through horizontal transfer of complete loci or individual modules, resulting in functional diversity (Mohanraju et al., 2016). To promote invasive potency, phages also produce inhibitors to enhance the ability to lyse host bacterium or effectively integrate into bacterial genomes (Mohanraju et al., 2016; Samson et al., 2013). Studies revealed that phages encode proteins to inhibit or directly interact with different Cas proteins to prevent

[1]State Key Laboratory of Trauma, Burns and Combined Injury, Institute of Surgery Research, Daping Hospital, The Third Military Medical University, Chongqing 400042, P. R. China

[2]Department of Biomedical Sciences, School of Medicine and Health Sciences, University of North Dakota, Grand Forks, ND 58203-9037, USA

[3]Biological Science Research Center, Southwest University, Chongqing 400715, P. R. China

[4]Key Laboratory of Biotechnology for Medicinal Plants of Jiangsu Province, Jiangsu Normal University, Xuzhou, Jiangsu 221116, P. R. China

[5]Key Laboratory of Resources Biology and Biotechnology in Western China, Ministry of Education, College of Life Science, Northwest University, Xi'an, ShaanXi 710069, P. R. China

[6]These authors contributed equally

[7]Lead Contact

*Correspondence: lianghh@nwu.edu.cn (H.L.), hellojjx@126.com (J.J.), min.wu@med.und.edu (M.W.)

https://doi.org/10.1016/j.isci.2019.02.005

the functionality of CRISPR-Cas systems (Bondy-Denomy et al., 2015; Rauch et al., 2017; Sontheimer and Davidson, 2017). However, little is presently known about whether CRISPR-Cas systems can be regulated by bacterial own genes.

Quorum sensing (QS) is known not only to govern bacterial virulence but also to regulate communication between bacterial cells and organize collective behaviors in bacterial populations (Papenfort and Bassler, 2016). Recently, QS signaling was found to mediate the expression and activity of multiple CRISPR-Cas systems (Høyland-Kroghsbo et al., 2017; Patterson et al., 2016). These QS effects on prokaryotic adaptive immune systems are strongly associated with cell density, because increased diversity of CRISPR spacers within communities restricts the success of phage escape mutants (van Houte et al., 2016). Modulating CRISPR-Cas immunity regulated by QS opens up a question of how bacterial signaling controls the CRISPR-Cas system, but how bacterial genes finely regulate CRISPR-Cas system at the molecular levels remains uncertain (Hofer, 2017; Marraffini, 2017; Semenova and Severinov, 2016). We recently identified a novel QS regulator, CdpR (ClpAP-degradation and pathogenicity regulator), which negatively modulates the *Pseudomonas* quinolone signal (PQS) system in PAO1 strain (Zhao et al., 2016). PQS plays a role in the regulation of multiple genes involved in bacterial QS (Bredenbruch et al., 2006; Hassett et al., 1999). PQS and QS along with a group of transcriptional regulators form a complex regulatory network (Coggan and Wolfgang, 2012). However, whether CdpR can directly alter QS levels and function remains elusive. Furthermore, whether CdpR can influence the expression, activity, and immunity of CRISPR-Cas is completely unknown.

Here, we explored the role of CdpR in type I-F CRISPR-Cas system with *Pseudomonas aeruginosa* UCBPP-PA14 strain (denoted PA14) and reveal that CdpR represses the immunization and immunity potency of CRISPR-Cas via QS to impede the expression, activity, and spacer acquisition of the CRISPR-Cas system. The CdpR-mediated regulation of CRISPR-Cas influences phage infection by Vfr-mediated *cas1* promoter binding and expression. Hence, we propose that CdpR may prevent bacterial self-reactivity via blockade of CRISPR-mediated endogenous cleavage. These findings enlist CdpR as the first endogenous negative regulator of CRISPR-Cas systems to maintain the balance between host defense and self-targeting of CRISPR-Cas systems. Together, our studies highlight the role of precise regulation of CRISPR-Cas in the co-evolution of bacteria with their invaders, phages, to maintain an active host defense without harming their own genes.

RESULTS

CdpR Represses the Activity of CRISPR-Cas Interference and Spacer Acquisition

Recent studies imply that both bacterial genes and intracellular signals may regulate the expression and function of CRISPR-Cas. Since CdpR is a newly discovered regulator of QS genes and the QS systems can regulate CRISPR-Cas, we hypothesize that CdpR may modulate type I-F CRISPR-Cas systems in the PA14 strain. As expected, compared with the PA14-WT strain, the signal-deficient *cdpR* mutant (PA14-Δ*cdpR*) exhibited increased expression of Cas surveillance complex (Figure 1A). In agreement, expression of the Cas surveillance complex by complementation with CdpR (PA14-Δ*cdpR*/*p-cdpR*) was restored to the PA14-WT level. This result demonstrated that the expression of CRISPR-Cas loci is downregulated by CdpR.

To determine whether the function of CRISPR-Cas systems is also modulated by CdpR, we measured the effect of CRISPR-Cas on eliminating CRISPR-targeted or CRISPR-untargeted plasmid in the PA14-Δ*cdpR* strain. We generated two CRISPR-targeted plasmids, CR1-sp1 and CR2-sp1 (Cady et al., 2012), that possess a targeted protospacer (a sequence complementary to a spacer in CRISPR array 1 or 2, respectively) flanked by a cognate PAM (Figure 1B). We quantified the retention of plasmids in the PA14-WT and PA14-Δ*cdpR* strains with shaking for 5 h according to a previous report (Høyland-Kroghsbo et al., 2017). There was no loss of untargeted plasmid in all strains (Figure S1A), whereas loss of CR1-sp1 and CR2-sp1 plasmids occurred in PA14-WT, PA14-Δ*cdpR*, and PA14-Δ*cdpR*/*p-cdpR* compared with PA14-ΔTCR lacking *cas* genes (Figure S1B), indicating that plasmid loss resulted from CRISPR-Cas interference, consistent with the previous reports that CRISPR-Cas systems are required for foreign DNA interference (Barrangou et al., 2007; Marraffini and Sontheimer, 2008). Meanwhile, this loss was significantly influenced by CdpR, showing that CdpR inhibits the efficiency of CRISPR-Cas-mediated interference (Figure S1B). We investigated whether CdpR influences CRISPR-Cas-mediated elimination of an incoming genetic element that resembles a phage attack, which can be assessed by plasmid transformation efficiency of the PA14-WT and mutant strains. The transformation inhibition in the PA14-Δ*cdpR* strain was more efficient than that

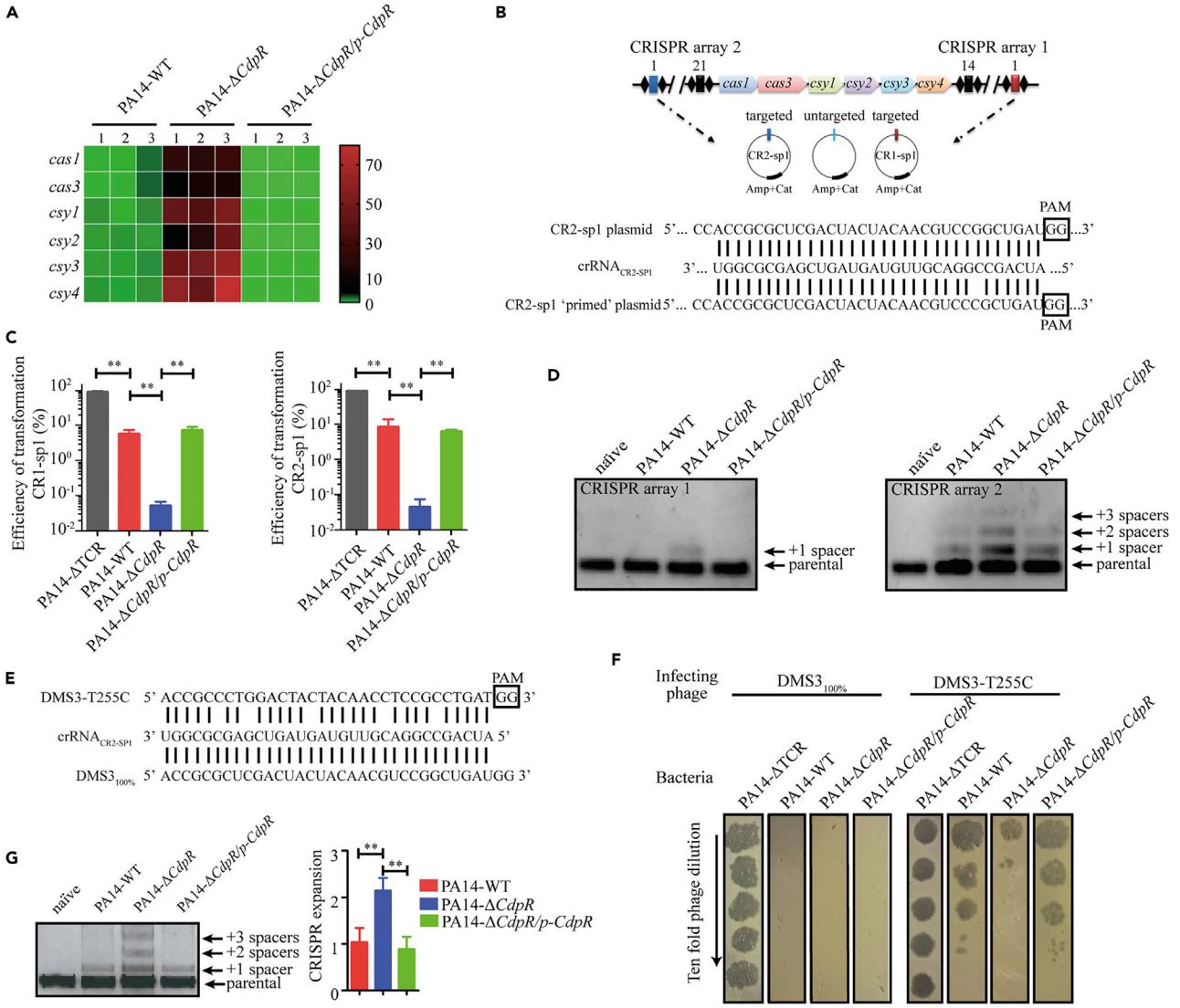

Figure 1. CdpR Represses the Activity of CRISPR-Cas System against Phage Infection

(A) Heatmap for *csy1-4*, *cas1*, and *cas3*-related mRNA transcripts in *P. aeruginosa* PA14-WT, PA14-Δ*cdpR*, and PA14-Δ*cdpR/p-cdpR* with the same cell density quantified by qRT-PCR. Data were normalized with 16sRNA expression as an internal control.

(B) The type I-F CRISPR-Cas locus in PA14. Experiments utilizing a non-targeted plasmid and two CRISPR-targeted plasmids (denoted CR1-sp1 and CR2-sp1) that contain a protospacer matching spacer 1 in CRISPR array 1 and 2, respectively.

(C) Transformation efficiency of CRISPR-targeted plasmids in PA14-WT or PA14-Δ*cdpR* mutant.

(D) New spacer acquisition (CRISPR expansion) in CRISPR array 1 or 2 locus evaluated by PCR in PA14-WT and mutant strains. Strains harbored the primed plasmid containing a seed mutation to promote adaptation. Naïve represents the native CRISPR arrays in the PA14 genome.

(E) Diagram of $crRNA_{CR2\text{-}sp1}$ in *P. aeruginosa* PA14 type I-F CRISPR-Cas systems interacting with DMS3-T255C and $DMS3_{100\%}$ sequences. Lines denote Watson-Crick base pairing between $crRNA_{CR2\text{-}sp1}$ and its phage target sequences in the DMS3-T255C and $DMS3_{100\%}$. PAM is shown within a shadowed box.

(F) $DMS3_{100\%}$ and DMS3-T255C phages grew on bacterial lawns of PA14-WT, PA14-Δ*cdpR*, PA14-Δ*cdpR/p-cdpR*, and PA14-ΔTCR.

(G) Acquisition of new spacer sequences with phage DMS3-T255C infection in PA14-WT and mutant strains analyzed by qPCR.

Data shown are the means ±SEM (n = 3) (one-way ANOVA plus Tukey test, $^{**}p < 0.01$; $^{*}p < 0.05$).

in the PA14-WT strain. In addition, complementation of *cdpR* restored the repression of CRISPR-Cas activity (Figure 1C). Collectively, these results affirm that CdpR represses CRISPR-Cas immunity, thereby hampering host defense against invasive elements.

Next, we questioned whether spacer acquisition is also regulated by CdpR. As the frequency of spacer acquisition can be increased by challenging bacteria with protospacer containing elements or primed

process (Datsenko et al., 2012), we constructed a primed plasmid by inserting a protospacer that targets CRISPR array 2 spacer 1 containing a single base mutation (Figure 1B). We detected new spacer acquisition in the CRISPR array locus and found that, although spacer acquisition occurred in both the PA14-WT and PA14-Δ*cdpR* strains, adaptation in the PA14-Δ*cdpR* mutant was increased vs. the PA14-WT strain, which was reversed to the WT level in the complemented strain, PA14-Δ*cdpR*/*p-cdpR* (Figures 1D and S1C). This result suggests that CdpR represses CRISPR-Cas activity and blocks spacer acquisition. In addition, we found that the adaptation frequency on the CRISPR array 2 locus was higher than that on the CRISPR array 1 locus (Figures 1D and S1C), consistent with a previous study (Westra et al., 2015). Collectively, these findings clearly establish that CdpR is a negative regulator for inhibiting the expression, interference, and adaptation of *P. aeruginosa* CRISPR-Cas systems.

CdpR-Deletion Mutation Enhances CRISPR-Cas-Mediated Immunity against Phage Invasion

CRISPR-Cas systems are important for bacteria to defend against phage invasion. To assess whether CdpR plays a role in phage infection, we measured plaque-forming efficiency of CRISPR-sensitive phage DMS3-T255C and $DMS3_{100\%}$ bearing a protospacer that is partially or completely (100%) complementary to the spacer portion of $crRNA_{CR2\text{-}sp1}$ in PA14 (Figure 1E), whereas wild-type DMS3 phage is CRISPR-insensitive (Cady et al., 2012). Phage $DMS3_{100\%}$ failed to replicate on the PA14-WT, PA14-Δ*cdpR*, and PA14-Δ*cdpR*/*p-cdpR* strains because of the adaptive immunity of CRISPR-Cas systems but was able to replicate on the CRISPR-Cas deficient PA14-ΔTCR strain (Figure 1F). The DMS3-T255C phage on the PA14-WT strain could form plaques robustly, whereas the $DMS3_{100\%}$ displayed at least a 10,000-fold lower plaque efficiency than the DMS3-T255C (Cady et al., 2012). Notably, we observed a low plaquing efficiency of DMS3-T255C on the PA14-Δ*cdpR* compared with that on the PA14-WT strain (Figure 1F). Remarkably, expression of the *cdpR* gene led to a marked increase in the plaquing efficiency of DMS3-T255C. Furthermore, new spacer acquisition was increased in the PA14-Δ*cdpR* strain compared with the PA14-WT strain (Figure 1G). Taken together, these data indicate that *cdpR*-deficiency mutation attenuates plaquing efficiency owing to its production of more potent CRISPR-Cas activity and that CdpR also negatively regulated CRISPR-Cas function during phage infection.

CdpR Represses CRISPR-Cas Regulation via QS Signals

CdpR was identified as a virulence regulator of the PQS in *P. aeruginosa* PAO1 strain missing CRISPR-Cas systems (Zhao et al., 2016). Bacteria communicate through QS systems to coordinate cooperative behaviors, which is essential for population fitness and invasion of hosts. We speculated that the QS circuit is associated with CdpR's effects on CRISPR-Cas systems in PA14 strains. Previous reports indicate that bacterial strains use chemical communication via QS systems to modulate CRISPR-Cas (Høyland-Kroghsbo et al., 2017; Patterson et al., 2016). In agreement, the QS circuit regulates the type I-F CRISPR-Cas systems by adjusting the expression of multiple Cas surveillance complexes at a high cell density in PA14 strains (Figures S2A and S2B). Furthermore, there were significantly increased QS-dependent transcripts of *lasI*/*rhlI* and other regulators (*bfiS*, *bfiR*, *bfmS*, *bfmR*, *exsA*, *gacS*, *gacA*, *hptB*, *rpoS*, and *sagS*, whose accumulation is associated with QS systems at a high cell density) in the PA14-Δ*cdpR* mutant compared with the PA14-WT strain, but these were restored to the WT levels in the P14-Δ*cdpR*/*p-cdpR* strain (Figure S2C). These responsive genes are diverse ranging from QS regulation to T3SS and small RNA regulators. We postulate that CdpR may repress adaptive immunity of CRISPR-Cas loci through QS signaling. To test this notion, we used the QS inhibitor baicalein (Luo et al., 2016) to treat the PA14-Δ*cdpR* background strain, not QS inhibitor meta-bromo-thiolactone (mBLT) owing to binding and inhibiting LasR and RhlR that showed no change in the *cdpR* mutant strain compared with the WT strain (Figure S2C). Interestingly, baicalein abolished the positive effect of QS signals on *cas* modules and altered *csy* expression (Figures 2A and S3A). Furthermore, the interference capability of these two target plasmids on the CdpR-dependent CRISPR-Cas activity was also inhibited by baicalein (Figures S3B and S3C). Moreover, the QS inhibitor affected CdpR-mediated transformation inhibition (Figure 2B). Finally, to address whether QS systems regulate spacer acquisition by CRISPR-Cas systems, we found that baicalein inhibited the efficiency of CRISPR adaptation to acquire new spacers via CdpR (Figures 2C and S3D), indicating that CdpR-mediated reduction of CRISPR-Cas activity represses the generation of immune memory by halting spacer acquisition through inhibition of QS systems. Collectively, these results imply that CdpR-mediated QS signaling is required for the control of CRISPR-Cas activity in PA14.

We further investigated whether CdpR-mediated regulation of CRISPR-Cas systems is dependent on QS regulators LasI/RhlI. Double mutations of Δ*lasI*/Δ*rhlI* negatively affected the expression of *cas* genes

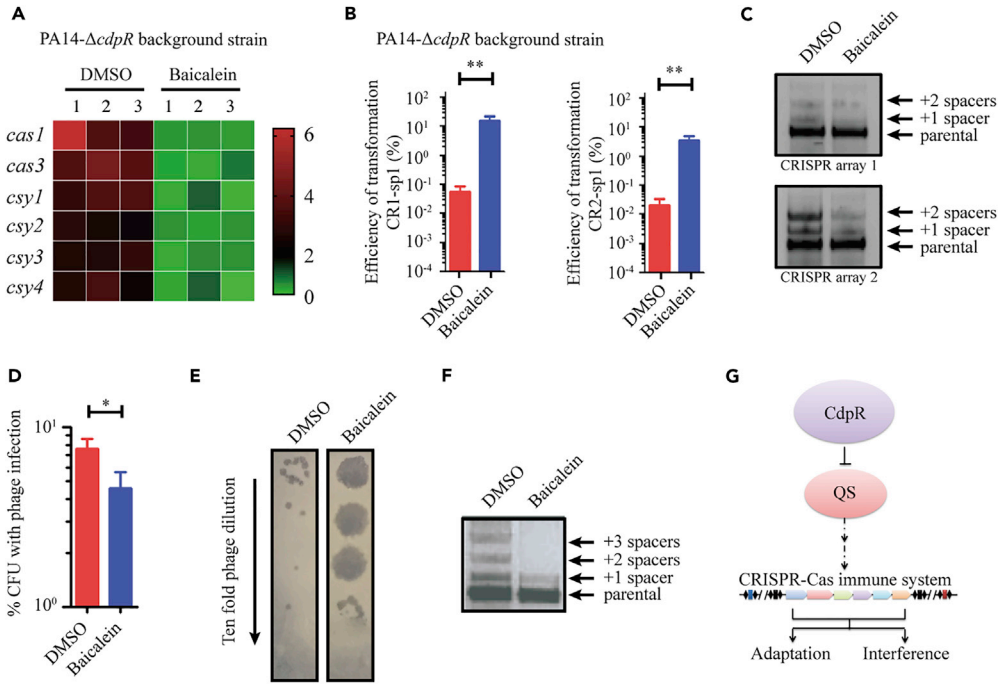

Figure 2. CdpR Mediates Repression of CRISPR-Cas System via Quorum Sensing

(A) Heatmap for CRISPR-Cas expression in PA14-Δ*cdpR* background with or without 100 μM QS inhibitor baicalein.

(B) Transformation efficiency of PA14-Δ*cdpR* background at high cell density with or without baicalein.

(C) Integration of new spacers into CRISPR loci was detected in PA14-Δ*cdpR* strains with or without baicalein.

(D) Retention assay of transformation efficiency of phage DMS3-T255C infection with PA14-Δ*cdpR* background with baicalein.

(E) Ability of phage DMS3-T255C to infect *cdpR*-deficiency mutant strains with or without baicalein.

(F) Integration of new spacers into a CRISPR array locus of PA14-Δ*cdpR* strain detected by PCR in the presence or absence of baicalein.

(G) Schematic of CdpR represses CRISPR-Cas immune response, including immunization and immunity, via QS.

Data shown are the means ± SEM (n = 3) (one-way ANOVA plus Tukey test, **p < 0.01; *p < 0.05).

(Figure S4A), consistent with the previous report (Høyland-Kroghsbo et al., 2017). We generated two Δ*cdpR*/Δ*lasI*, Δ*cdpR*/Δ*rhlI* double mutants and one Δ*cdpR*/Δ*lasI*/Δ*rhlI* triple mutant in the PA14 background. The increase of *cas1*, *cas3*, and *csy1-4* expression in PA14-Δ*cdpR* was abolished by double deletion of *lasI*/*rhlI* (Figure S4B). Furthermore, compared with that in the PA14-Δ*cdpR* strain, expansion of CRISPR arrays (Figure S4C) and interference of CRISPR-Cas systems (Figure S4D) were decreased in the PA14-Δ*cdpR*/Δ*lasI*/Δ*rhlI* strain. Collectively, these findings imply that CdpR-mediated QS signaling, especially LasI/RhlI, is required for the control of CRISPR-Cas activity in PA14.

To assess the relationship between QS systems and the consequences of CdpR on CRISPR-Cas function in phage infection, we detected the effect of CdpR on CRISPR-Cas function in the presence or absence of the QS inhibitor. Colony forming units (CFUs) of PA14-Δ*cdpR* treated with baicalein showed a 1.654-fold reduction of transformation efficiency compared with DMSO-treated controls (Figure 2D). Moreover, the plaquing efficiency of DMS3-T255C on the baicalein-treated PA14-Δ*cdpR* mutant was higher than that of DMSO-treated controls (Figure 2E). In addition, inhibiting QS signaling reduced the spacer acquisition in the PA14-Δ*cdpR* strain following DMS3-T255C infection (Figure 2F). These results indicate that QS participates in the inhibition of CdpR in CRISPR-Cas function against phage infection. Taken together, our findings suggest that CdpR broadly represses CRISPR-Cas immune responses, including immunization and immunity, via QS signaling to resist phage infection (Figure 2G).

Vfr Is Required for Regulating CRISPR-Cas Systems by CdpR

P. aeruginosa possesses one of the most sophisticated QS systems of all bacterial species, which coordinate a group of transcriptional regulators (such as VqsR, QscR, VqsM, Vfr, and RpoN) to form a complex

regulatory network (Coggan and Wolfgang, 2012). To explore the mechanism of how CdpR controls CRISPR-Cas adaptive immunity via the QS signaling, we performed bioinformatic analysis of the consensus-binding motif of these QS transcription regulators in the promoter region of *cas* operon and found a putative *v*irulence *f*actor *r*egulator (Vfr)-binding *cis*-response elements (CREs) in the *cas1* promoter that are homologous to the Vfr consensus-binding site (5′-ANWWTGNGAWNYAGWTCACAT-3′) (Fuchs et al., 2010) (Figure 3A). We identified that Vfr is essential for modulating adaptation and interference (Figures 3B–3D). Both phages $DMS_{100\%}$ and DMS3-T255C showed lower plaquing efficiency on the PA14-WT strain than on the PA14-Δ*vfr* strain (Figure 3E), indicating that Vfr regulated CRISPR-Cas immunity during phage infection. Vfr was previously implicated in the regulation of a wide range of promoters (Fuchs et al., 2010). To further test whether Vfr regulates the *cas* operon, we investigated *cas1* promoter activity in the PA14-WT and PA14-Δ*vfr* strains in the entire growth period. Remarkably, the *cas1* promoter activity was significantly reduced in the PA14-Δ*vfr* strain (Figure 3F) and complementation of *vfr* to the PA14-Δ*vfr* mutant restored to the levels of the WT strain (Figure 3G), indicating that Vfr can activate *cas1* promoter. To determine whether Vfr directly controls *cas1* promoter activity, we designed and generated a *cas1* promoter-fragment to perform electrophoretic mobility shift assay (EMSA) with the recombinant His-Vfr proteins. Incubation of the *cas1* promoter with increasing amounts Vfr proteins resulted in the dose-dependent formation of the Vfr/*cas1* promoter complex (Figure 3H), demonstrating that Vfr directly binds to the *cas1* promoter. Thus, we designed oligonucleotide probes for these sites or mutated the binding motifs (Figure 3A). EMSA analysis revealed that Vfr bound to the WT Vfr CRE but not to the mutant Vfr CRE (Figures 3G and 3I). To further evaluate whether the Vfr CRE is required for the activation of the *cas1* promoter, we mutated the binding sites in the *cas1* promoter region. Our results showed that activation of the *cas1* promoter was abolished with the mutant Vfr CRE compared with a *lacZ* reporter possessing the intact Vfr CRE in the PA14-WT strain (Figure 3G). Taken together, these results demonstrate that Vfr requires the specific Vfr CRE to activate the *cas* operon, which is responsible for the functionality of type I-F CRISPR-Cas in PA14.

Deletion of CdpR in PA14 exhibited a pronounced increase in the expression of *vfr* compared with the WT strain (Figure 4A). To further investigate the influence of Vfr in the CdpR-mediated CRISPR-Cas function, PA14-Δ*cdpR*, PA14-Δ*vfr* single mutant, and PA14-Δ*cdpR*/Δ*vfr* double mutant strains were generated and the expression of the CRISPR-Cas system was quantified in these strains. The increase of *cas1*, *cas3*, *csy1-4* expression and *cas1* promoter activity in PA14-Δ*cdpR* were abolished by deletion of *vfr*, but complementation of *vfr* to the PA14-Δ*cdpR*/Δ*vfr* mutant restored to the WT-PA14 or PA14-Δ*cdpR* levels (Figures 4B and 4C), indicating that Vfr profoundly influences the CdpR-mediated regulation of the CRISPR-Cas system. Furthermore, transformation efficiency analysis demonstrated that CRISPR-Cas interference was decreased in the PA14-Δ*cdpR*/Δ*vfr* strain compared with the PA14-Δ*cdpR* strain but restored to the control level by vfr complementation (PA14-Δ*cdpR*/Δ*vfr*/*p-vfr* strain, Figure 4D). Moreover, expansion of the CRISPR array was not detectable in the PA14-Δ*cdpR*/Δ*vfr* strain compared with the PA14-WT and PA14-Δ*cdpR* strains (Figure 4E). Taken together, these data elucidate that CdpR connects Vfr to regulate the interference and spacer acquisition by type I-F CRISPR-Cas systems (Figure 4F).

QS LasI/RhlI Participate in the CdpR/Vfr-Mediated Regulation of CRISPR-Cas Functionality

We investigated whether Vfr affects the CdpR-mediated regulation of CRISPR-Cas system via QS (LasI/RhlI) and found that the Δ*lasI*/Δ*rhlI* double mutant negatively impacted *cas1* promoter activity (Figure 5A). The enhanced activity of *cas1* promoter in the PA14-Δ*cdpR* was abolished by double deletion of *lasI*/*rhlI* (Figure 5B). In addition, the expression of *vfr* was markedly increased by adding QS autoinducers: 3OC12-HSL and C4-HSL (Figure 5C), whereas baicalein blocked this effect of QS signals, resulting in a modest reduction in *vfr* expression compared with the WT strain (Figure 5C). Similarly, the *cas1* promoter activity was enhanced by the QS autoinducers but decreased by the QS inhibitor baicalein (Figure 5D). Furthermore, the increase of *cas1* promoter activity was abolished by the autoinducers when Vfr CRE was mutated (Figure 5D). These results strongly indicate that QS signals regulate Vfr to positively influence the *cas* operon. Since LasI and RhlI synthesize 3OC12-HSL and C4-HSL, respectively (Papenfort and Bassler, 2016), we delved into the relationship of LasI/RhlI with Vfr. As expected, disruption of *lasI*/*rhlI* attenuated *vfr* expression (Figure 5E). Addition of 3OC12-HSL and C4-HSL to the cultured PA14-Δ*lasI*/Δ*rhlI* strain increased *vfr* expression (Figure 5F), which is consistent with reduction of the *cas* operon activity in the absence of LasI/RhlI (Figures 5A and 5G). These findings proved that LasI and RhlI help in the production of QS autoinducers to activate *vfr*. Collectively, our data indicate that CdpR represses QS regulators to achieve the modulation of CRISPR-Cas functionality in a Vfr-dependent manner (Figure 5H).

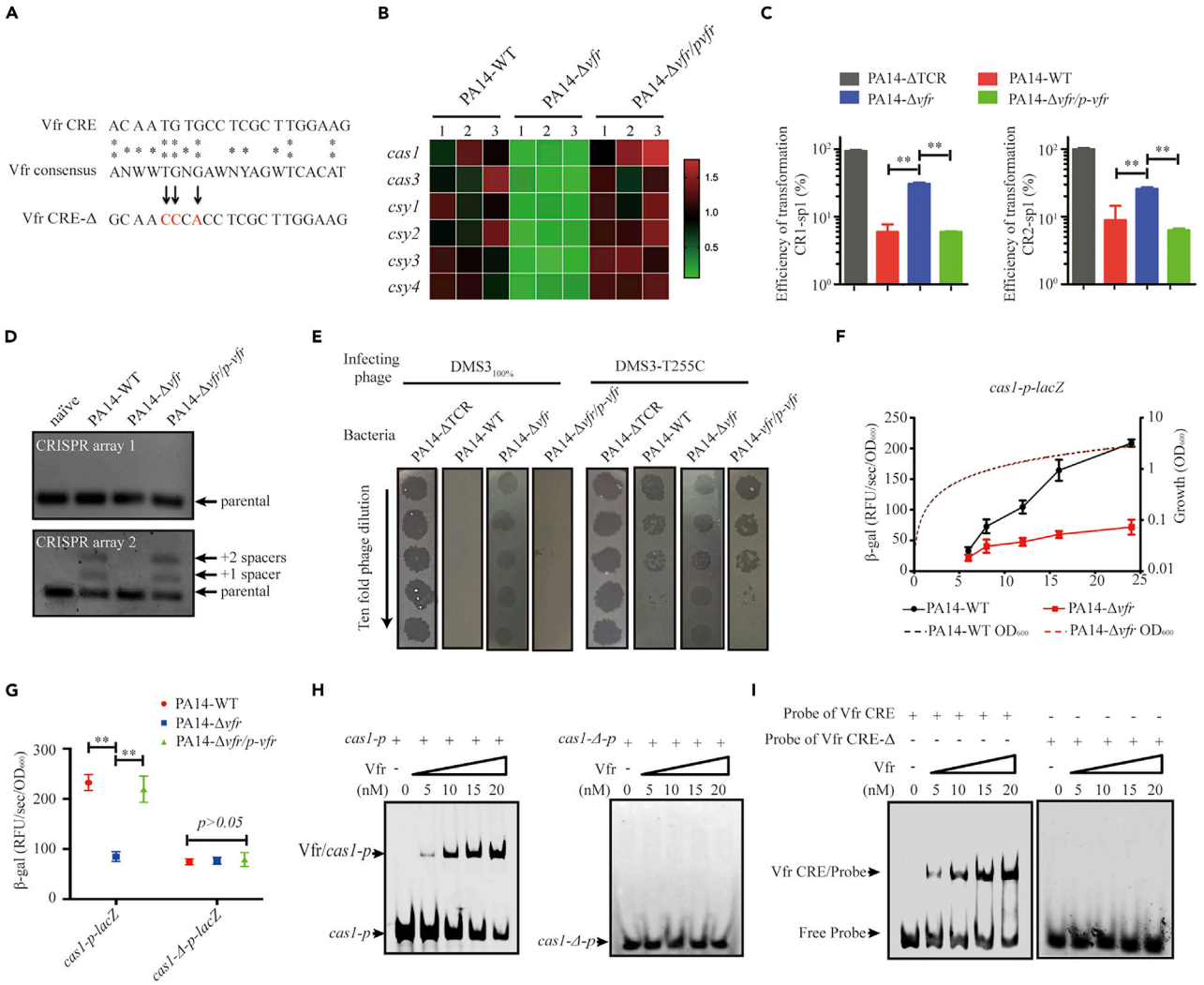

Figure 3. Vfr Promotes CRISPR-Cas Activities by Binding CRISPR-Cas Promoter Operon

(A) The PA14 *cas1* promoter contains a *cis*-response element (CRE) similar to Vfr-binding consensus site in *P. aeruginosa* PAO1. A mutated CRE shown in red for investigating Vfr binding (Vfr CRE-Δ). Star represents bases matching the consensus.

(B) Heatmap for relative transcripts of *cas1*, *cas3*, and *csy1-4* in PA14-WT, PA14-Δ*vfr*, and PA14-Δ*vfr/p-vfr* quantified by qRT-PCR. Data were normalized with 16sRNA expression as an internal control.

(C) Transformation efficiency of CRISPR-targeted plasmids in the PA14-WT or PA14-Δ*vfr* mutant.

(D) New spacer acquisition (CRISPR expansion) in CRISPR array 1 or 2 locus was quantified in PA14-WT, PA14-Δ*vfr*, and PA14-Δ*vfr/p-vfr* mutant strains by PCR-based analysis.

(E) $DMS3_{100\%}$ and DMS3-T255C phages grew on bacterial lawns of PA14-WT, PA14-Δ*vfr*, PA14-Δ*vfr/p-vfr*, and PA14-ΔTCR.

(F) Expression of the integrative *cas1-p-lacZ* for *cas* operon reporter in PA14-WT and PA14-Δ*vfr* mutant. Dashed lines indicate growth in lysogeny broth (LB); solid lines represent *cas1* promoter activity.

(G) Expression of the *cas1* promoter or the *cas1* promoter containing mutated Vfr-binding sites (*cas1*-Δ-*p*) in the PA14-WT, PA14-Δ*vfr*, or PA14-Δ*vfr/p-vfr* mutant measured at 24 h.

(H) EMSA for binding of Vfr to the *cas* operon. Left, interaction between Vfr and *cas1* promoter; right, mutation analysis of the Vfr-binding site in *cas1* promoter binding to Vfr.

(I) EMSA for Vfr binds to the region of Vfr CRE or CRE-Δ probe.

Data shown are the means ± SEM (n = 3) (one-way ANOVA plus Tukey test, **p < 0.01; *p < 0.05).

CdpR Inhibits CRISPR-Cas Systems to Regulate Endogenous Transcription

Running a constantly active CRISPR-Cas system imposes a risk of cleaving the bacterial own mRNA or DNA as a CRISPR spacer may happen to be partially complementary to their own sequences, which may lead to autoimmunity. Based on the mechanism of RNA binding for PA14 CRISPR-Cas systems as recently

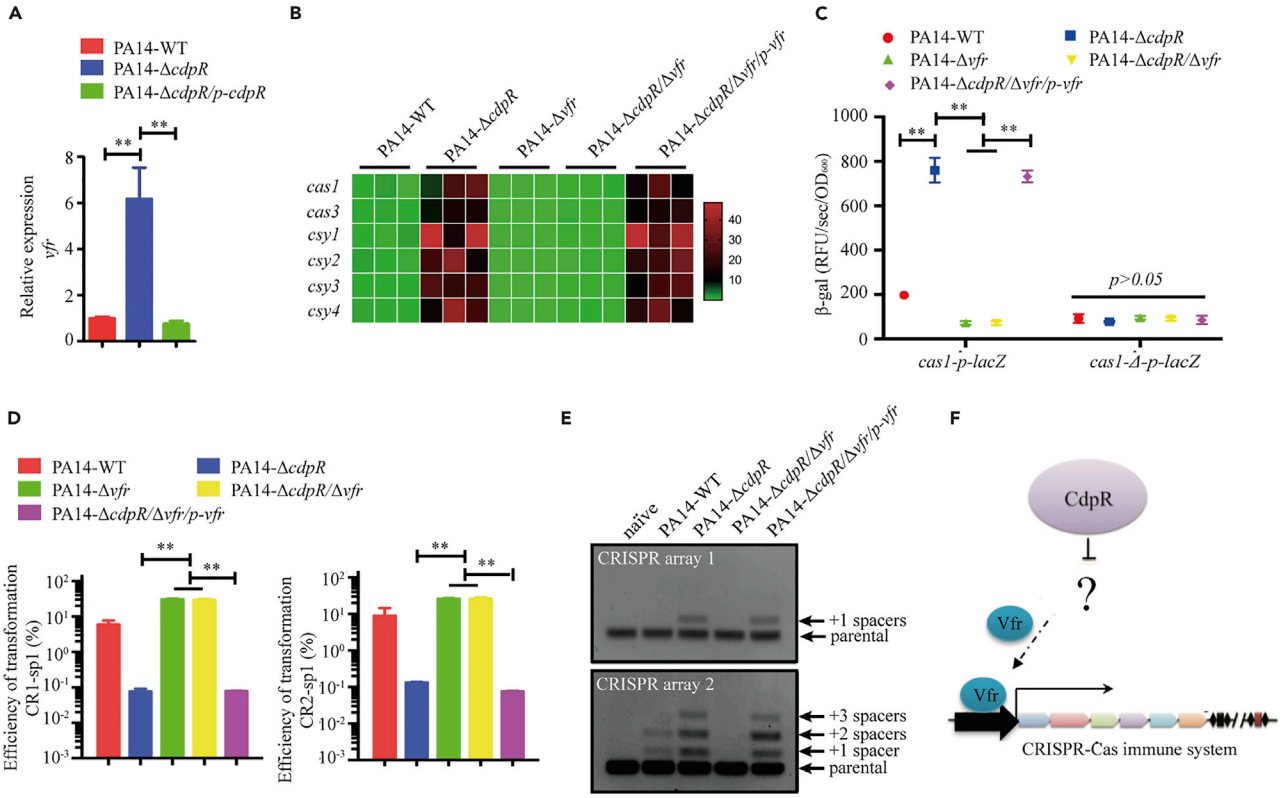

Figure 4. Vfr along with CdpR Modulates Activity of CRISPR-Cas Loci through Binding Cas Promoter

(A) qRT-PCR analysis of *vfr* in PA14-WT, PA14-Δ*cdpR*, and PA14-Δ*cdpR/p-cdpR*.

(B) Heatmap for *cas*-related transcripts in PA14-WT, PA14-Δ*cdpR*, PA14-Δ*vfr*, PA14-Δ*cdpR*/Δ*vfr*, and PA14-Δ*cdpR*/Δ*vfr/p-vfr*.

(C) *cas1-p-lacZ* and *cas1*-Δ-*p-lacZ* activity in the PA14-WT, PA14-Δ*cdpR*, PA14-Δ*vfr*, PA14-Δ*cdpR*/Δ*vfr*, and PA14-Δ*cdpR*/Δ*vfr/p-vfr* mutant strains were measured at 24 h post inoculation.

(D) Transformation efficiency of CRISPR-targeted plasmids in the PA14-WT or mutant strains.

(E) Integration of new spacers into CRISPR array loci detected in PA14-Δ*cdpR* strains with or without the deletion of *vfr*.

(F) Schematic of the CdpR cooperating with Vfr to control CRISPR-Cas system functionality.

Bars, means ± SEM; n = 3; **p < 0.01; *p < 0.05 (one-way ANOVA plus Tukey test).

described (Li et al., 2016; Müller-Esparza and Randau, 2017), the crRNAs of type I-F CRISPR-Cas system in PA14 may potentially target 189 endogenous transcripts (Figure 6A and Table S1). To investigate whether CdpR-mediated alterations of CRISPR-Cas affect endogenous genes at the transcription level, we probed crRNA-guided recognition of *glpF* and *cysT* mRNA based on 5′-GGN-3′ of PAM near its 5′-end but not 3′-end among these 189 candidate endogenous transcripts, which may be potentially recognized by PA14 CRISPR-Cas (Figures 6B and S5). The PA14-ΔTCR mutant strain lacking *cas* genes showed increased transcripts of *glpF* or *cysT* compared with the PA14-WT strain, but this was restored similarly to the WT levels in the complemented strain PA14-ΔTCR/p-TCR. These results argue that CRISPR-Cas systems are indeed involved in the targeted regulation of endogenous genes. Furthermore, the expression of *glpF* or *cysT* transcripts was markedly repressed in PA14-Δ*cdpR* compared with the PA14-WT strain but was not changed in PAO1-Δ*cdpR* compared with the PAO1-WT strain (Figures 6B and S5A) that does not possess CRISPR-Cas systems and serves as another negative control. We then examined the expression of *phzM*, which is not a target for the crRNAs, as additional control, and found that it had not been altered in the different strains (Figure S5B).

To precisely gauge the capacity for endogenous RNA targeting by CRISPR-Cas, we employed a co-immunoprecipitation (Co-IP) approach combined with northern blot analysis (Figure 6C). The *cas3* gene was tagged with 6xHis in PA14-WT, PA14-Δ*cdpR*, and PA14-Δ*cdpR/p-ΔcdpR* strains. We performed a Co-IP on the *cas3*-6xHis strains (Figures 6C and S5C, lanes 4–6) and the untagged strains as a control (Figures 6C and S5C, lanes 1–3) to obtain RNA for northern blot. We identified *glpF* and

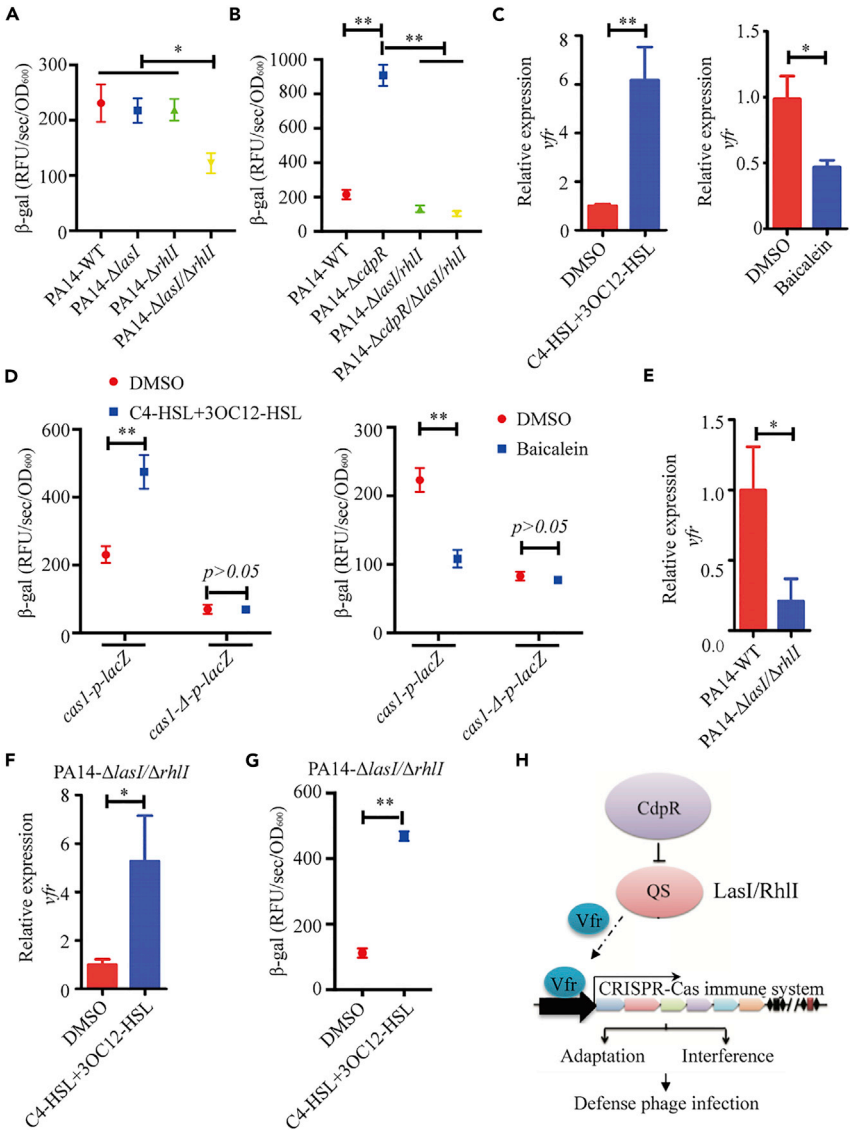

Figure 5. QS LasI/RhlI Participate in CdpR-Mediated Regulation of CRISPR-Cas System via Vfr

(A) Expression of *cas1-p-lacZ* reporter in PA14-WT, PA14-Δ*lasI*, PA14-Δ*rhlI*, and PA14-Δ*lasI*/Δ*rhlI* at 24 h post inoculation.

(B) *cas1-p-lacZ* activity in PA14-WT, PA14-Δ*cdpR*, and PA14-cdpR/ΔlasI/ΔrhlI backgrounds at 24 h post inoculation.

(C) qRT-PCR analysis of vfr in PA14-WT with or without QS autoinducers (2 μM 3OC12-HSL and 10 μM C4-HSL) or inhibitor (100 μM baicalein).

(D) Expression of the integrative *cas1-p-lacZ* and *cas1*-Δ-*p-lacZ* for *cas* operon reporter in PA14-WT in the presence or absence of QS autoinducers or inhibitor.

(E) Relative transcripts of *vfr* in PA14-WT and PA14-Δ*lasI*/Δ*rhlI* quantified by qRT-PCR.

(F) qRT-PCR analysis of *vfr* in the PA14-Δ*lasI*/Δ*rhlI* background with or without QS autoinducers.

(G) Expression of the integrative *cas1-p-lacZ* for *cas* operon reporter in PA14-Δ*lasI*/Δ*rhlI* mutant in the absence or presence of QS autoinducers.

(H) Schematic of CdpR repressing QS regulators LasI/RhlI to inhibit CRISPR-Cas system functionality via Vfr.

Bars, means ± SEM; n = 3; **p < 0.01; *p < 0.05 (one-way ANOVA plus Tukey test).

cysT mRNA fragments with enrichment in Cas3-6xHis Co-IP (Figures 6C, left and S5C, lane 4) but found no change in *phzM* serving as a negative control (Figure 6C, right), indicating that Cas3 directly binds to endogenous RNA. Moreover, northern blot showed that endogenous transcripts of *glpF* or *cysT* were more abundant in the PA14-Δ*cdpR* strain than in the WT strain (Figures 6C-left and S5C, lanes 4–6). Moreover, similar results for the detection of crRNA binding to Cascade complex were observed via

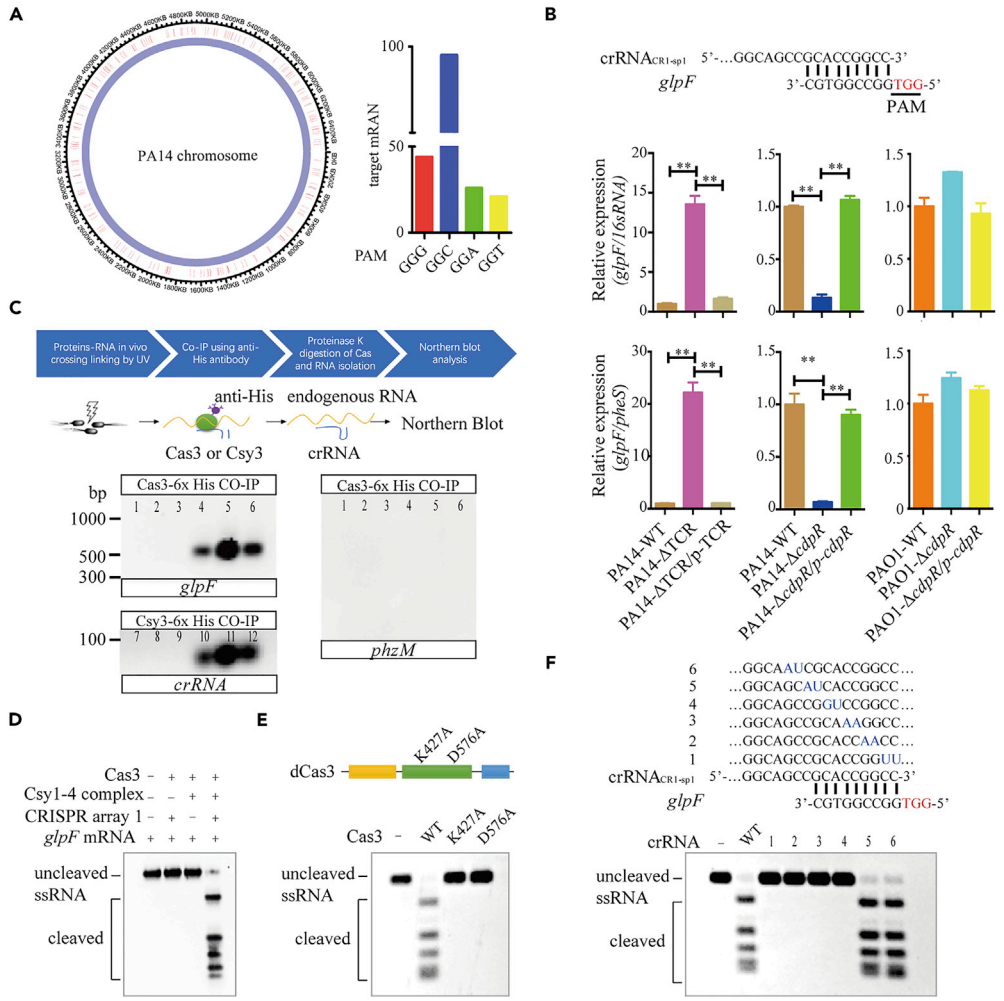

Figure 6. CdpR Inhibits Endogenous RNA Cleavage Mediated by CRISPR-Cas

(A) Graphical representation of the targeted position of PA14 crRNA spacers in the genome (orange). Rectangular columns show the number of spacers matching the mRNA of endogenous genes.

(B) Homology comparison between the mRNA sequences of endogenous genes (*glpF*) and CRISPR array 1 spacer 1 in PA14-WT. Transcripts of endogenous genes in PA14-WT and mutant strains at the same cell density quantified by qPCR. Data were normalized with 16sRNA or housekeeping gene *pheS* expression as an internal control.

(C) Overview of Co-IP with anti-His tag antibody combined with northern blot to identify endogenous transcripts binding to the CRISPR-Cas system. Northern blot analysis of *glpF* mRNA in the indicated strains (1: PA14-WT; 2: PA14-Δ*cdpR*; 3: PA14-Δ*cdpR/p-cdpR*; 4: PA14-WT/cas3-6xHis; 5: PA14-Δ*cdpR/cas3-6xHis*; 6 PA14-Δ*cdpR/p-cdpR*/cas3-6xHis; 7: PA14-WT; 8: PA14-Δ*cdpR*; 9: PA14-Δ*cdpR/p-cdpR*; 10: PA14-WT/*csy3-6xHis*; 11: PA14-Δ*cdpR/csy3-6xHis*; 12 PA14-Δ*cdpR/p-cdpR*/csy3-6xHis). RNAs determined with radiolabeled oligonucleotide probes.

(D) Single-strand glpF RNA subjected to *in vitro* digestion by purified, recombinant Cas3 and Csy complex.

(E) Nuclease-dead Cas3 has no effect on *glpF* mRNA cleavage.

(F) Effect of crRNA-target RNA mismatch on the seed-region base-pairing sitting with glpF mRNA subjected to *in vitro* digestion by Cas3-Csy complexes.

Data shown are the means ± SEM (n = 3) (one-way ANOVA plus Tukey test; $^{**}p < 0.01$; $^{*}p < 0.05$).

Csy3-6xHis Co-IP (Figure 6C). In addition, cleavage assay showed that a significant amount of *glpF* mRNAs were cleaved *in vitro* by the CRISPR-Cas complex (Figure 6D). However, glpF mRNA substrates were not cleaved by nuclease-dead Cas3 (K427A or D576A mutants in DExD/H domain) (Figure 6E). We also found that the seed-region base-pairing between crRNA and RNA substrates is critical for RNA cleavage, as mutation of these nucleotides results in reduced glpF mRNA cleavage (Figure 6F). Taken together, these studies suggest that CdpR maintains the endogenous transcripts stabilization by inhibiting the activity of CRISPR-Cas. Overall, these findings demonstrate that CRISPR-mediated repression of

endogenous transcripts may be neutralized by CdpR, which may be critical for regulating the abundance of individual mRNA and shaping bacterial transcriptomes.

DISCUSSION

To date, knowledge about the microbial CRISPR-mediated adaptive immunity is rapidly evolving, particularly its primary function in preventing phage infection (Marraffini, 2015). Invasion and expansion of phages are likely to occur with the increase of bacterial cell density and can be monitored by QS surveying (Knowles et al., 2016). We uncover that CdpR facilitates the repression of CRISPR-Cas loci via regulation of QS systems. Consistent with this finding, the *cdpR*-deficiency mutant strain exhibits enhanced CRISPR-Cas immunity via QS signaling against phages' or foreign MGEs' invasion, indicating that CdpR-repressed QS signals, especially combination with LasI/RhlI axis, modulate the anti-phage mechanism during infection. In short, CdpR together with QS signals adds another layer of organization to bacterial anti-phage intracellular signaling. These analyses also suggest that bacterial intrinsic anti-QS components, such as CdpR, may amplify the risk of viral infection, which reflects the critical virulence ability for QS systems in invasion of hosts, consistent with that self-targeting may be harmful to bacteria (Briner and Barrangou, 2016).

Vfr functions as a global regulator of virulence factors in response to environmental cues (Coggan and Wolfgang, 2012). Vfr positively regulates the production of type IV pili (Tfp), type III secretion system (T3SS), and LasR QS system that control the expression of hundreds of additional genes (Albus et al., 1997; Sadikot et al., 2005). In addition, Vfr negatively regulates flagellar gene expression (Coggan and Wolfgang, 2012). We noticed that a consensus Vfr binding sequence located in the *cas* operon region interacts with Vfr to alter expression levels of CRISPR-Cas systems. Furthermore, Vfr is required for the CdpR-mediated regulation of CRISPR-Cas immune function. Moreover, the function of Vfr was activated by QS autoinducers and repressed by QS inhibitors. These data illustrate that CdpR represses QS regulators to inhibit CRISPR-Cas immunity through the Vfr signaling; however, the detailed mechanism remains to be defined.

CRISPR-Cas adaptive immunity widely exists in the bacterial world because of the everlasting viruses-host arm race and/or collaboration (Mohanraju et al., 2016). However, the expression of CRISPR-Cas loci is costly because of the possibility of self-targeting between the spacer and portion of the endogenous genes in the genome that is not part of a CRISPR array (Dugar et al., 2018; Li et al., 2016). *P. aeruginosa* type I-F CRISPR-Cas systems (Cas3) are reported to cleave the *lasR* RNA, resulting in an impaired immune response by the host (Li et al., 2016). In accordance, suppression of both *P. aeruginosa* biofilm formation and swarming motility by its type I-F CRISPR-Cas system requires the crRNA (Heussler et al., 2015). Furthermore, mutation of the *Myxococcus xanthus* type I-C CRISPR-Cas system leads to reduced expression of the FruA response regulator, resulting in markedly impaired sporulation (Boysen et al., 2002; Viswanathan et al., 2007). *Listeria monocytogenes* type I-A CRISPR-Cas systems enhance virulence by promoting the expression of a ferrous iron transporter (Mandin et al., 2007; Toledo-Arana et al., 2009). Moreover, a constantly active CRISPR-Cas system increases chances of accidental incorporation of nucleic acids from the cell's own genome to incur self-reactivity and even death (Stern et al., 2010). The burden of CRISPR-Cas systems, such as targeting endogenous RNA/DNA through imperfect complementarity with crRNA guides and cleavage by Cas nucleases, might provide selective pressure to co-evolution of bacteria against CRISPR-Cas adaptive immunity. Since CdpR is a newly discovered repressor that provides inhibitory effects on CRISPR-Cas function, especially inhibition of CRISPR-mediated endogenous mRNA target, it is highly likely that bacteria need to finely tune CRISPR-Cas activity to provide sufficient host defense while minimizing risk of self-targeting.

Discriminating self from non-self to effectively block invaders is a universal requirement of immune systems to function normally without self-destruction. CRISPR-Cas immunity requires a sequence match between invasive nucleic acids and spacers for cleavage of foreign DNA (Marraffini, 2015; van Houte et al., 2016), and recognition of PAM serves as a mechanism for self- and non-self-discrimination during type I-F CRISPR-Cas interference (Hayes et al., 2016; Kieper et al., 2018; Sashital et al., 2012; Westra et al., 2012, 2013). Hence, the PAM sequence of CRISPR motifs is important for new spacer acquisition (Wang et al., 2015). The sequence of PAM such as Cas3 5′-GG-3′ is widespread in *P. aeruginosa* chromosomes (Rollins et al., 2015). However, the fact is that only about one bacterium in 10 million will gain a spacer from bacterial chromosomal DNA incorporated into CRISPR loci to defend itself (Stern et al., 2010). This suggests that there is an unknown mechanism to repress the efficiency of CRISPR-Cas systems to acquire spacers from self-genome or exert cell signaling to mediate appropriate CRISPR-Cas function. The CRISPR-Cas immunity is tightly controlled, especially limiting spacer integration, providing one approach to decreasing

self-targeting (Marraffini, 2017; Stern et al., 2010). Our results demonstrate that CdpR represses immunization and immunity of CRISPR-Cas systems, suggesting that bacteria may have evolved a variety of mechanisms to reduce the risk of spacer acquisition from bacterial chromosomal DNA. Inhibiting self-targeting resembles negative immune-regulation or immune tolerance in mammals as a surveillance mechanism to prevent severe tissue destruction or chronic diseases. However, how the self/non-self-discrimination is regulated remains to be fully studied (Ledford, 2017; Mohanraju et al., 2016).

In conclusion, our results demonstrate the importance of bacterial intracellular signaling in coordinating adaptive immunity in prokaryotes. This study puts forward a previously unrecognized mechanism for the regulation of CRISPR-Cas defense systems by CdpR, where an internal negative mediator has not been identified. Our proposed model delineates a series of events that are associated with CdpR action. In this model, CdpR, as a repressor, inhibits the expression and function of CRISPR-Cas systems by hampering the stimulation of QS and Vfr signaling during bacterial defense against MGEs or phages. Furthermore, CdpR inhibits CRISPR-mediated bacterial endogenous cleavage to reduce the risk of self-targeting, which needs to be further investigated. Nevertheless, our study provides the first account on how bacteria utilize virulence regulators to down-regulate CRISPR immune capacity thereby maintaining homeostasis. The negative regulatory mechanism of CRISPR-Cas systems helps balance effective host defense and self-repression by CRISPR-Cas activities. Hence, this fine-tuning of CRISPR-Cas prevents self-targeting to avoid potential autoimmunity and even mortality, while maintaining a robust CRISPR-Cas adaptive immunity.

Limitations of the Study

In this study, we identify the first intrinsic negative regulator for CRISPR-Cas that directly impacts functional activities of interference and adaptation, which keeps homeostasis while efficiently counteracting ruthless invasion by bacteriophage. However, we also made a number of observations that are intriguing but need to be probed further experimentally: whether CdpR interacts with a protein or binds to nucleic acids involved in CRISPR-Cas immunity; if so, how does it work with Vfr to control the CRISPR-Cas system. Furthermore, it remains unclear how CdpR controls QS signals and which domain is required for this mechanism. Moreover, it is currently unknown if other regulators can promote or repress the activity of CRISPR-Cas adaptive immunity. Finally, whether the possible mechanistic model of Cas3/Csy complexes-mediated RNA cleavage executes new potential function remains to be defined.

METHODS

All methods can be found in the accompanying Transparent Methods supplemental file.

SUPPLEMENTAL INFORMATION

Supplemental Information includes Transparent Methods, five figures, and five tables and can be found with this article online at https://doi.org/10.1016/j.isci.2019.02.005.

ACKNOWLEDGMENTS

We thank Dr. George A. O'Toole of Dartmouth Medical School for providing strains and phages, Dr. Bonnie L. Bassler of Princeton University for providing QS mutants, Dr. Peter C. Fineran of University of Otago for providing the *lacZ* reporter, Dr. Lennart Randau at Max Planck Institute for Terrestrial Microbiology for providing the data about the targeted gene for PA14 crRNA spacers, and Dr. Sergei Nechaev of University of North Dakota for revising the manuscript. This work was supported by the National Institutes of Health, United States (AI101973-01, AI109317-01A1, and AI097532-01A1 to M.W); this work was also supported by the Key Program of National Nature Science Foundation of China, China (81530063 to J.J.). The funders had no role in study design, data collection and analysis, decision to publish, or preparation of the manuscript.

AUTHOR CONTRIBUTIONS

P.L., M.W., and J.X.J. designed the project and wrote the manuscript. P.L. and Q.P. designed and performed most of the experiments. H.L. provided important reagents. P.L., M.W., and J.X.J analyzed data. G.S., R.L., K.G., C.Z., and H.L. advised on experimental design and manuscript preparation.

DECLARATION OF INTERESTS

The authors declare no competing interests.

Received: May 7, 2018
Revised: September 26, 2018
Accepted: February 6, 2019
Published: March 29, 2019

REFERENCES

Albus, A.M., Pesci, E.C., Runyen-Janecky, L.J., West, S., and Iglewski, B.H. (1997). Vfr controls quorum sensing in *Pseudomonas aeruginosa*. J. Bacteriol. *179*, 3928–3935.

Barrangou, R., Fremaux, C., Deveau, H., Richards, M., Boyaval, P., Moineau, S., Romero, D.A., and Horvath, P. (2007). CRISPR provides acquired resistance against viruses in prokaryotes. Science *315*, 1709–1712.

Bondy-Denomy, J., Garcia, B., Strum, S., Du, M., Rollins, M.F., Hidalgo-Reyes, Y., Wiedenheft, B., Maxwell, K.L., and Davidson, A.R. (2015). Multiple mechanisms for CRISPR-Cas inhibition by anti-CRISPR proteins. Nature *526*, 136–139.

Boysen, A., Ellehauge, E., Julien, B., and Søgaard-Andersen, L. (2002). The DevT protein stimulates synthesis of FruA, a signal transduction protein required for fruiting body morphogenesis in *Myxococcus xanthus*. J. Bacteriol. *184*, 1540–1546.

Bredenbruch, F., Geffers, R., Nimtz, M., Buer, J., and Haussler, S. (2006). The *Pseudomonas aeruginosa* quinolone signal (PQS) has an iron-chelating activity. Environ. Microbiol. *8*, 1318–1329.

Briner, A.E., and Barrangou, R. (2016). Deciphering and shaping bacterial diversity through CRISPR. Curr. Opin. Microbiol. *31*, 101–108.

Burstein, D., Harrington, L.B., Strutt, S.C., Probst, A.J., Anantharaman, K., Thomas, B.C., Doudna, J.A., and Banfield, J.F. (2017). New CRISPR–Cas systems from uncultivated microbes. Nature *526*, 136–139.

Cady, K.C., Bondy-Denomy, J., Heussler, G.E., Davidson, A.R., and O'Toole, G.A. (2012). The CRISPR/Cas adaptive immune system of *Pseudomonas aeruginosa* mediates resistance to naturally occurring and engineered phages. J. Bacteriol. *194*, 5728–5738.

Coggan, K.A., and Wolfgang, M.C. (2012). Global regulatory pathways and cross-talk control *Pseudomonas aeruginosa* environmental lifestyle and virulence phenotype. Curr. Issues Mol. Biol. *14*, 47–70.

Datsenko, K.A., Pougach, K., Tikhonov, A., Wanner, B.L., Severinov, K., and Semenova, E. (2012). Molecular memory of prior infections activates the CRISPR/Cas adaptive bacterial immunity system. Nat. Commun. *3*, 945.

Deltcheva, E., Chylinski, K., Sharma, C.M., Gonzales, K., Chao, Y., Pirzada, Z.A., Eckert, M.R., Vogel, J., and Charpentier, E. (2011). CRISPR RNA maturation by trans-encoded small RNA and host factor RNase III. Nature *471*, 602–607.

Dugar, G., Leenay, R.T., Eisenbart, S.K., Bischler, T., Aul, B.U., Beisel, C.L., and Sharma, C.M. (2018). CRISPR RNA-dependent binding and cleavage of endogenous RNAs by the campylobacter jejuni Cas9. Mol. Cell *69*, 893–905.e7.

East-Seletsky, A., O'Connell, M.R., Knight, S.C., Burstein, D., Cate, J.H., Tjian, R., and Doudna, J.A. (2016). Two distinct RNase activities of CRISPR-C2c2 enable guide-RNA processing and RNA detection. Nature *538*, 270–273.

Fonfara, I., Richter, H., Bratovič, M., Le Rhun, A., and Charpentier, E. (2016). The CRISPR-associated DNA-cleaving enzyme Cpf1 also processes precursor CRISPR RNA. Nature *532*, 517–521.

Fuchs, E.L., Brutinel, E.D., Jones, A.K., Fulcher, N.B., Urbanowski, M.L., Yahr, T.L., and Wolfgang, M.C. (2010). The *Pseudomonas aeruginosa* Vfr regulator controls global virulence factor expression through cyclic AMP-dependent and -independent mechanisms. J. Bacteriol. *192*, 3553–3564.

Garneau, J.E., Dupuis, M.-È., Villion, M., Romero, D.A., Barrangou, R., Boyaval, P., Fremaux, C., Horvath, P., Magadán, A.H., and Moineau, S. (2010). The CRISPR/Cas bacterial immune system cleaves bacteriophage and plasmid DNA. Nature *468*, 67–71.

Hassett, D.J., Ma, J.F., Elkins, J.G., McDermott, T.R., Ochsner, U.A., West, S.E., Huang, C.T., Fredericks, J., Burnett, S., Stewart, P.S., et al. (1999). Quorum sensing in *Pseudomonas aeruginosa* controls expression of catalase and superoxide dismutase genes and mediates biofilm susceptibility to hydrogen peroxide. Mol. Microbiol. *34*, 1082–1093.

Hayes, R.P., Xiao, Y., Ding, F., van Erp, P.B., Rajashankar, K., Bailey, S., Wiedenheft, B., and Ke, A. (2016). Structural basis for promiscuous PAM recognition in type I-E Cascade from E. coli. Nature *530*, 499–503.

Heler, R., Samai, P., Modell, J.W., Weiner, C., Goldberg, G.W., Bikard, D., and Marraffini, L.A. (2015). Cas9 specifies functional viral targets during CRISPR-Cas adaptation. Nature *519*, 199–202.

Heussler, G.E., Cady, K.C., Koeppen, K., Bhuju, S., Stanton, B.A., and O'Toole, G.A. (2015). Clustered regularly interspaced short palindromic repeat-dependent, biofilm-specific death of *Pseudomonas aeruginosa* mediated by increased expression of phage-related genes. MBio *6*, e00129–00115.

Hofer, U. (2017). Bacterial physiology: quorum sensing controls the cost of CRISPR-Cas. Nat. Rev. Microbiol. *15*, 2–3.

Høyland-Kroghsbo, N.M., Paczkowski, J., Mukherjee, S., Broniewski, J., Westra, E., Bondy-Denomy, J., and Bassler, B.L. (2017). Quorum sensing controls the *Pseudomonas aeruginosa* CRISPR-Cas adaptive immune system. Proc. Natl. Acad. Sci. U S A *114*, 131–135.

Kieper, S.N., Almendros, C., Behler, J., McKenzie, R.E., Nobrega, F.L., Haagsma, A.C., Vink, J.N.A., Hess, W.R., and Brouns, S.J.J. (2018). Cas4 facilitates PAM-compatible spacer selection during CRISPR adaptation. Cell Rep. *22*, 3377–3384.

Knowles, B., Silveira, C., Bailey, B., Barott, K., Cantu, V., Cobián-Güemes, A., Coutinho, F., Dinsdale, E., Felts, B., and Furby, K. (2016). Lytic to temperate switching of viral communities. Nature *531*, 466–470.

Koonin, E.V., Makarova, K.S., and Wolf, Y.I. (2017). Evolutionary genomics of defense systems in archaea and bacteria. Annu. Rev. Microbiol. *71*, 233–261.

Labrie, S.J., Samson, J.E., and Moineau, S. (2010). Bacteriophage resistance mechanisms. Nat. Rev. Microbiol. *8*, 317–327.

Ledford, H. (2017). Five big mysteries about CRISPR's origins. Nature *541*, 280–282.

Lewis, K.M., and Ke, A. (2017). Building the class 2 CRISPR-Cas arsenal. Mol. Cell *65*, 377–379.

Li, R., Fang, L., Tan, S., Yu, M., Li, X., He, S., Wei, Y., Li, G., Jiang, J., and Wu, M. (2016). Type I CRISPR-Cas targets endogenous genes and regulates virulence to evade mammalian host immunity. Cell Res. *26*, 1273–1287.

Luo, J., Kong, J.-L., Dong, B.-Y., Huang, H., Wang, K., Wu, L.-H., Hou, C.-C., Liang, Y., Li, B., and Chen, Y.-Q. (2016). Baicalein attenuates the quorum sensing-controlled virulence factors of Pseudomonas aeruginosa and relieves the inflammatory response in *P. aeruginosa*-infected macrophages by downregulating the MaPK and nFκB signal-transduction pathways. Drug Des. Devel. Ther. *10*, 183.

Makarova, K.S., Wolf, Y.I., Alkhnbashi, O.S., Costa, F., Shah, S.A., Saunders, S.J., Barrangou, R., Brouns, S.J., Charpentier, E., and Haft, D.H. (2015). An updated evolutionary classification of CRISPR-Cas systems. Nat. Rev. Microbiol. *13*, 722–736.

Mandin, P., Repoila, F., Vergassola, M., Geissmann, T., and Cossart, P. (2007). Identification of new noncoding RNAs in Listeria monocytogenes and prediction of mRNA targets. Nucleic Acids Res. *35*, 962–974.

Marraffini, L.A. (2015). CRISPR-Cas immunity in prokaryotes. Nature *526*, 55–61.

Marraffini, L.A. (2017). Sensing danger. Proc. Natl. Acad. Sci. U S A *114*, 15–16.

Marraffini, L.A., and Sontheimer, E.J. (2008). CRISPR interference limits horizontal gene transfer in staphylococci by targeting DNA. Science *322*, 1843–1845.

McGinn, J., and Marraffini, L.A. (2016). CRISPR-cas systems optimize their immune response by

specifying the site of spacer integration. Mol. Cell *64*, 616–623.

Mohanraju, P., Makarova, K.S., Zetsche, B., Zhang, F., Koonin, E.V., and van der Oost, J. (2016). Diverse evolutionary roots and mechanistic variations of the CRISPR-Cas systems. Science *353*, aad5147.

Müller-Esparza, H., and Randau, L. (2017). Comment: type I CRISPR-Cas targets endogenous genes and regulates virulence to evade mammalian host immunity. Front Microbiol. *8*, 319.

Papenfort, K., and Bassler, B.L. (2016). Quorum sensing signal-response systems in Gram-negative bacteria. Nat. Rev. Microbiol. *14*, 576–588.

Patterson, A.G., Jackson, S.A., Taylor, C., Evans, G.B., Salmond, G.P.C., Przybilski, R., Staals, R.H.J., and Fineran, P.C. (2016). Quorum sensing controls adaptive immunity through the regulation of multiple CRISPR-Cas systems. Mol. Cell *64*, 1102–1108.

Rauch, B.J., Silvis, M.R., Hultquist, J.F., Waters, C.S., McGregor, M.J., Krogan, N.J., and Bondy-Denomy, J. (2017). Inhibition of CRISPR-Cas9 with bacteriophage proteins. Cell *168*, 150–158.

Rollins, M.F., Schuman, J.T., Paulus, K., Bukhari, H.S., and Wiedenheft, B. (2015). Mechanism of foreign DNA recognition by a CRISPR RNA-guided surveillance complex from *Pseudomonas aeruginosa*. Nucleic Acids Res. *43*, 2216–2222.

Sadikot, R.T., Blackwell, T.S., Christman, J.W., and Prince, A.S. (2005). Pathogen–host interactions in *Pseudomonas aeruginosa* pneumonia. Am. J. Respir.Crit. Care Med. *171*, 1209–1223.

Samson, J.E., Magadán, A.H., Sabri, M., and Moineau, S. (2013). Revenge of the phages: defeating bacterial defences. Nat. Rev. Microbiol. *11*, 675–687.

Sashital, D.G., Wiedenheft, B., and Doudna, J.A. (2012). Mechanism of foreign DNA selection in a bacterial adaptive immune system. Mol. Cell *46*, 606–615.

Semenova, E., and Severinov, K. (2016). Come Together: CRISPR-Cas immunity senses the quorum. Mol. Cell *64*, 1013–1015.

Smargon, A.A., Cox, D.B., Pyzocha, N.K., Zheng, K., Slaymaker, I.M., Gootenberg, J.S., Abudayyeh, O.A., Essletzbichler, P., Shmakov, S., and Makarova, K.S. (2017). Cas13b is a Type VI-B CRISPR-associated RNA-Guided RNase differentially regulated by accessory proteins Csx27 and Csx28. Mol. Cell *65*, 1–13.

Sontheimer, E.J., and Davidson, A.R. (2017). Inhibition of CRISPR-Cas systems by mobile genetic elements. Curr. Opin. Microbiol. *37*, 120–127.

Stern, A., Keren, L., Wurtzel, O., Amitai, G., and Sorek, R. (2010). Self-targeting by CRISPR: gene regulation or autoimmunity? Trends Genet. *26*, 335–340.

Toledo-Arana, A., Dussurget, O., Nikitas, G., Sesto, N., Guet-Revillet, H., Balestrino, D., Loh, E., Gripenland, J., Tiensuu, T., Vaitkevicius, K., et al. (2009). The Listeria transcriptional landscape from saprophytism to virulence. Nature *459*, 950–956.

van Houte, S., Ekroth, A.K., Broniewski, J.M., Chabas, H., Ashby, B., Bondy-Denomy, J., Gandon, S., Boots, M., Paterson, S., and Buckling, A. (2016). The diversity-generating benefits of a prokaryotic adaptive immune system. Nature *532*, 385–388.

Viswanathan, P., Murphy, K., Julien, B., Garza, A.G., and Kroos, L. (2007). Regulation of dev, an operon that includes genes essential for *Myxococcus xanthus* development and CRISPR-associated genes and repeats. J. Bacteriol. *189*, 3738–3750.

Wang, J., Li, J., Zhao, H., Sheng, G., Wang, M., Yin, M., and Wang, Y. (2015). Structural and mechanistic basis of PAM-dependent spacer acquisition in CRISPR-cas systems. Cell *163*, 840–853.

Westra, E.R., Semenova, E., Datsenko, K.A., Jackson, R.N., Wiedenheft, B., Severinov, K., and Brouns, S.J. (2013). Type I-E CRISPR-cas systems discriminate target from non-target DNA through base pairing-independent PAM recognition. PLoS Genet. *9*, e1003742.

Westra, E.R., van Erp, P.B., Kunne, T., Wong, S.P., Staals, R.H., Seegers, C.L., Bollen, S., Jore, M.M., Semenova, E., Severinov, K., et al. (2012). CRISPR immunity relies on the consecutive binding and degradation of negatively supercoiled invader DNA by Cascade and Cas3. Mol. Cell *46*, 595–605.

Westra, E.R., van Houte, S., Oyesiku-Blakemore, S., Makin, B., Broniewski, J.M., Best, A., Bondy-Denomy, J., Davidson, A., Boots, M., and Buckling, A. (2015). Parasite exposure drives selective evolution of constitutive versus inducible defense. Curr. Biol. *25*, 1043–1049.

Zhao, J., Yu, X., Zhu, M., Kang, H., Ma, J., Wu, M., Gan, J., Deng, X., and Liang, H. (2016). Structural and molecular mechanism of CdpR involved in quorum-sensing and bacterial virulence in *Pseudomonas aeruginosa*. PLoS Biol. *14*, e1002449.

ISCI, Volume *13*

Supplemental Information

CdpR Inhibits CRISPR-Cas Adaptive Immunity to Lower Anti-viral Defense while Avoiding Self-Reactivity

Ping Lin, Qinqin Pu, Guanwang Shen, Rongpeng Li, Kai Guo, Chuanmin Zhou, Haihua Liang, Jianxin Jiang, and Min Wu

Supplemental Figures and legends

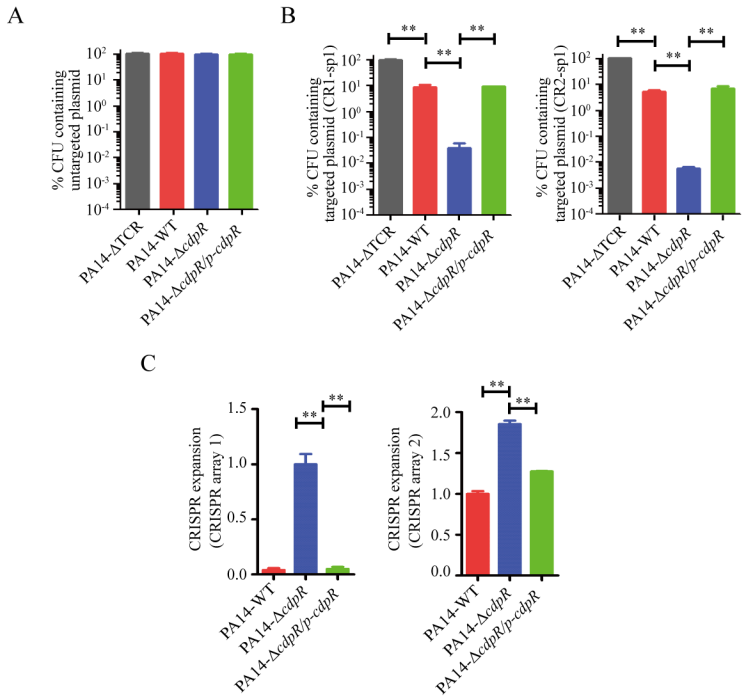

Figure S1. CdpR Represses the Activity of PA14 type I-F CRISPR-Cas Systems, related to Figure 1.
(A) Retention of the untargeted plasmid in PA14-WT, PA14-Δ*cdpR*, PA14-Δ*cdpR/p-CdpR*, and CRISPR-Cas system knockout strain (PA14-ΔTCR) during growth. (B) Plasmid-retention assay of the CRISPR-targeted plasmids (CR1-sp1 or CR2-sp1 spacers) in the PA14-WT or PA14-Δ*cdpR* mutant backgrounds. (C) Densitometric quantification of the immunoblotting gel data presented in Fig. 1D (in text) using ImageJ software. Data are representative of three experiments expressed as means ± SEM. Statistical significance was assessed by Using One way ANOVA plus Tukey test (**P<0.01; *P<0.05).

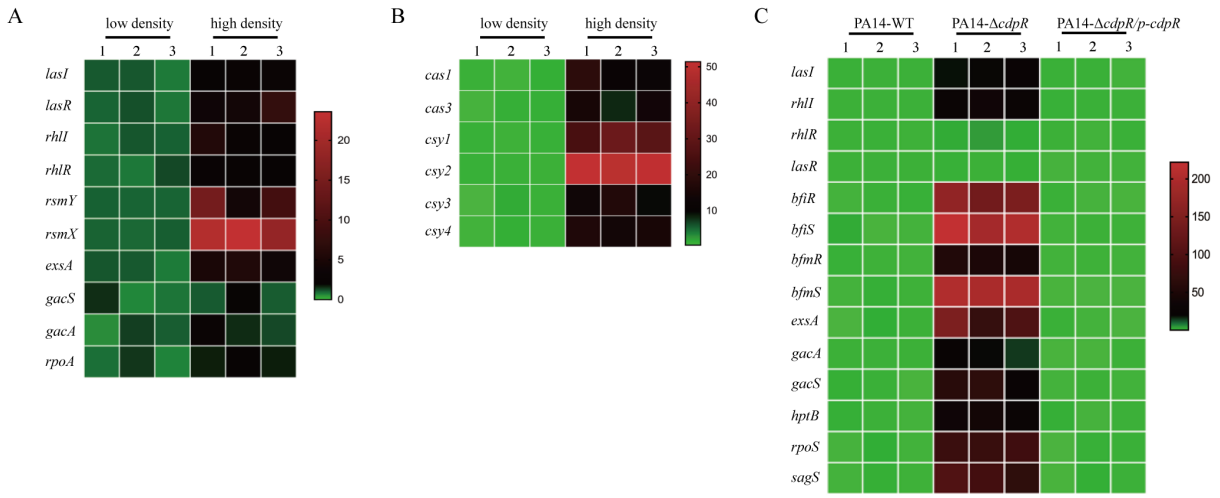

Figure S2. CdpR Regulates QS Systems to Inhibit the Expression of CRISPR-Cas System, related to Figure 2.

(A) Heat map for QS regulators in *P. aeruginosa* strain UCBPP-PA14 with low density (OD_{600}=0.1) and high density (OD_{600}=1) phases. (B) Heat map for relative expression of CRISPR-Cas locus by qRT-PCR analysis at low and high cell density. (C) Heat map for QS system regulators in wild-type PA14 (PA14-WT), *cdpR*-deficient strain (PA14-Δ*cdpR*), and its restored strain. The expression level of QS regulator lasR in *cdpR*-deficiency mutant strain.

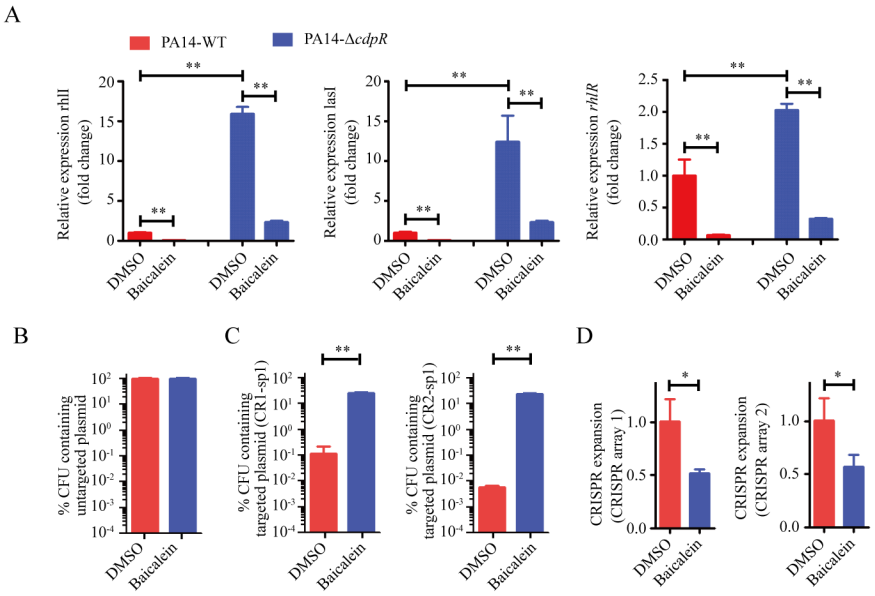

Figure S3. CdpR Represses the Activity of CRISPR-Cas Interference via QS, related to Figure 2.

(A) qPCR analysis of QS regulators *lasI*, *rhlI*, and *rhlR* in PA14-WT and PA14-Δ*cdpR* strains with or without QS inhibitor Baicalein. (B) Retention of the untargeted plasmid in PA14-Δ*cdpR* strain in the absence or presence of QS inhibitor Baicalein. (C) Plasmid-retention assay of the CRISPR-targeted plasmids (CR1-sp1 or CR2-sp1 spacers) in PA14-Δ*cdpR* strain with or without QS inhibitor Baicalein. (D) Densitometric quantification of the immunoblotting gel data presented in Fig. 1G (in text) using ImageJ software. Data are representative of three experiments expressed as means ± SEM. Statistical significance was assessed by Using One way ANOVA plus Tukey test (**P<0.01; *P<0.05).

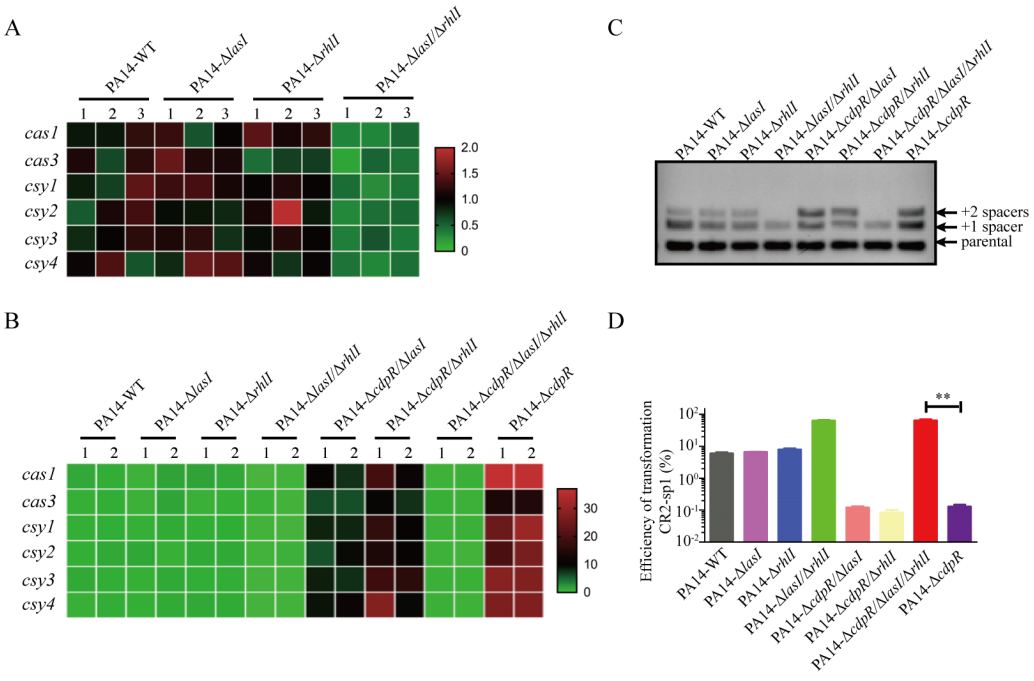

Figure S4. CdpR Represses the Activity of CRISPR-Cas Adaptation and Interference Involving LasI/RhlI, related to Figure 2.

(A) qPCR analysis of cas-related genes in the PA14-WT, PA14-Δ*lasI*, PA14-Δ*rhlI*, and PA14-Δ*lasI*/Δ*rhlI*. (B) Relative transcripts of *cas1*, *cas3*, and *csy1-4* were quantified by qRT-PCR in QS mutants background with the deletion of *cdpR*. (C) PCR-based analysis to check new spacer acquisition (CRISPR expansion) in CRISPR array 2 locus was quantified in PA14-WT and mutant strains that harbored the primed plasmid containing a seed mutation to promote adaptation. (D) Transformation efficiency of CRISPR-targeted plasmids in the PA14-WT or mutants. Data are representative of three experiments expressed as means ± SEM. Statistical significance was assessed by Using One way ANOVA plus Tukey test (**P<0.01; *P<0.05).

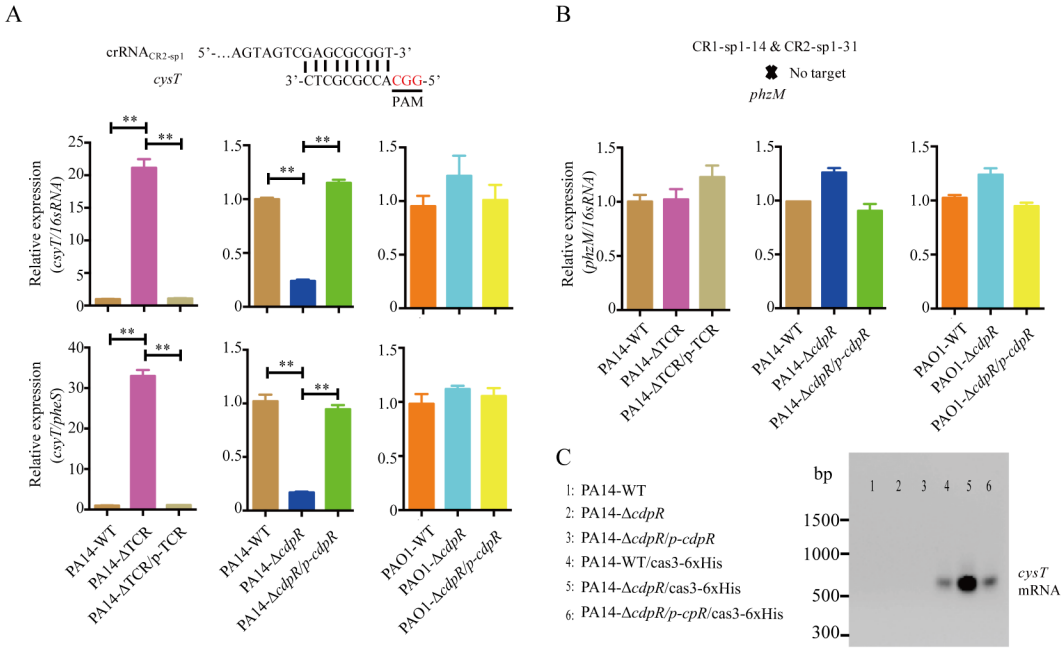

Figure S5. CdpR Inhibits mRNA Cleavage by CRISPR-Cas Systems, related to Figure 6.

(A) Homology comparison between the mRNA sequences of endogenous genes (*cysT*) and CRISPR array 2 spacer 1 in PA14-WT. Transcripts of endogenous genes in *P. aeruginosa* WT and mutant strains at the same cell density quantified by qPCR. Data were normalized with 16sRNA or housekeeping gene *pheS* expression as an internal control. (B) Transcripts of endogenous genes (*phzM*, no target by CRISPR-Cas loci) in *P. aeruginosa* WT and mutant strains at the same cell density quantified by qPCR. (C) Northern blot analysis of *cysT* mRNA in the indicated strains. RNAs were probe with radiolabeled oligonucleotide probes. Data were normalized with 16sRNA expression as an internal control. Data shown are the means ± SEM (n=3) (Using One way ANOVA plus Tukey test; **P<0.01; *P<0.05).

Supplemental Tables

Table S2. Bacterial strains, phage and plasmid used in this study, related to **Figure 1 to 6.**

Strain or Phage	Relevant characteristic	Reference or source
Bacteria strain		
E. coli	*E. coli* suitable for protein expression	New England Biolabs
PA14-WT	Wild-type *P. aeruginosa UCBPP-PA14* (PA14)	Laboratory stock
PA14-GFP	GFP label for *P. aeruginosa UCBPP-PA14*	Laboratory stock
PA14-Δ*CdpR*	PA14, CdpR deleting	Present study
PA14-Δ*CdpR*/*p-CdpR*	*CdpR* deleting, pAK1900-*CdpR*	Present study
PA14-ΔTCR	PA14, *cas* region deleting, pgRNA-crRNA1-14, crRNA1-21	Laboratory stock
PAO1-WT	Wild-type *P. aeruginosa PAO1*	Laboratory stock
PAO1-Δ*CdpR*	PAO1, *CdpR* deleting	(Jacobs et al., 2003)
PAO1-Δ*CdpR*/*p-CdpR*	*CdpR* deleting, pAK1900-*CdpR*	Present study
PA14-Δ*vfr*	PA14, *vfr* deleting	Present study
PA14-Δ*vfr*/*p-vfr*	*vfr* deleting, pAK1900-*vfr*	Present study
PA14-Δ*CdpR*/Δ*vfr*	PA14, double *CdpR*, *vfr* deleting	Present study
PA14-Δ*CdpR*/Δ*vfr*/*p-vfr*	double *CdpR*, *vfr* deleting, pAK1900-*vfr*	Present study
PA14-Δ*lasI*	PA14, *lasI* deleting	(Høyland-Kroghsbo et al., 2017)
PA14-Δ*rhlI*	PA14, *rhlI* deleting	(Høyland-Kroghsbo et al., 2017)
PA14-Δ*lasI*/Δ*rhlI*	PA14, double *lasI*, *rhlI* deleting	(Høyland-Kroghsbo et al., 2017)
PA14-Δ*CdpR*/Δ*lasI*	PA14, double *CdpR*, *lasI* deleting	Present study
PA14-Δ*CdpR*/Δ*rhlI*	PA14, double *CdpR*, *rhlI* deleting	Present study
PA14-Δ*CdpR*/Δ*lasI*/Δ*rhlI*	PA14, triple *CdpR*, *lasI*, *rhlI* deleting	Present study
PA14-WT/Cas3-6xHis	PA14, pMQ70-*cas3*His	Present study
PA14-Δ*CdpR* /Cas3-6xHis	PA14, CdpR deleting, pMQ70-*cas3*His	Present study
PA14-Δ*CdpR*/*p-CdpR* /Cas3-6xHis	PA14, pMQ70-*cas3*His	Present study
PA14-WT/csy3-6xHis	PA14, pMQ70-*csy3*His	Present study
PA14-Δ*CdpR* /csy33-6xHis	PA14, CdpR deleting, pMQ70-*csy3*His	Present study
PA14-Δ*CdpR*/*p-CdpR* /csy3-6xHis	PA14, pMQ70-*csy3*His	Present study

Bacteriophage		
DMS3-T255C	DMS3 with DMS3-42 T255C allele	(Cady et al., 2012)
DMS3-100%	DMS3 with 100% complementary to the spacer portion of $crRNA_{CR2\_sp1}$	(Cady et al., 2012)
Plasmid		
CRISPR-targeted CR1-sp1	CR1-sp1 plasmid containing the protospacer to CRISPR1 spacer 1	Present study
CRISPR-targeted CR2-sp1	CR2-sp1 plasmid containing the protospacer to CRISPR2 spacer 1	Present study
Primed CR1-sp1	CR1-sp1 plasmid containing the protospacer to CRISPR1 spacer 1 with a one base seed mutation	Present study
Primed CR2-sp1	CR2-sp1 plasmid containing the protospacer to CRISPR2 spacer 1 with a one base seed mutation	Present study
pgRNA	Expression of customizable guide RNA (gRNA)	Laboratory stock
pET-28a	*E. coli* expression vector	Laboratory stock
pET-28a-*vfr*	Vfr expression vector	Present study
pAK1900	*P. aeruginosa* expression vector	Laboratory stock
pAK1900-*CdpR*	CdpR expression vector	Present study
pAK1900-*vfr*	Vfr expression vector	Present study
pCVD442	*P. aeruginosa* gene knockout vector	Laboratory stock
pKO-*CdpR*	pCVD442-*CdpR*-flank	Present study
pKO-*vfr*	pCVD442-*vfr*-flank	Present study
pVIK107-Tc	integrative lacZ reporter plasmid	(Patterson et al., 2016)
cas1-p-lacZ	*cas1-p-lacZ* reporter	Present study
cas1-Δ-*p-lacZ*	*cas1*-Δ-*p-lacZ* reporter	Present study
pMQ70	Arabinose-inducible expression vector	(Zegans et al., 2009)
pMQ70-*cas3*His	PA14-cas3-6xHis vector	Laboratory stock
pMQ70-*csy3*His	PA14-csy3-6xHis vector	Present study

Table S3. Oligonucleotides for plasmids construction used in this study, related to **Figure 1 to 4**.

Name	sequences
Primer P1	5’-CGGGATCC GATATCTGGCGAAAATGAGAC-3’
Primer P2	5’-TGCACTGCAG TCAGATAAAATATTTCTAGATTTCA-3’
Primer P3	5’-AGCTCCACCACCCGCTACCACCGGCAGCCGCACCGGCCCC-3’
Primer P4	5’-GATCGGGGCCGGTGCGGCTGCCGGTGGTAGCGGGTGGTGG-3’
Primer P5	5’-AGCTGGACCGCGCTCGACTACTACAACGTCCGGCTGATGG-3’
Primer P6	5’-GATCCCATCAGCCGGACGTTGTAGTAGTCGAGCGCGGTCC-3’
Primer P7	5’-AGCTGGACCGCGCTCGACTACTACAACGTCCGCCTGATGG-3’
Primer P8	5’-GATCCCATCAGGCGGACGTTGTAGTAGTCGAGCGCGGTCC-3’
Primer P9	5’-AGAGGGTTTTTCCGGGCT-3’
Primer P10	5’-CCAGCGCGCCGGTGAT-3’
Primer P11	5’-GAGGGTTTCTGGCGGGAA-3’
Primer P12	5’-GTCCAGAAGTCACCACCCG-3’
Primer P13	5'-CGAGCTCGGACAGCCCACCGACCCTA-3'
Primer P14	5'-GGGGAATCATGCCGGCGGTTACCTCTTGCAGCG-3'
Primer P15	5'–TGCAAGAGGTAACCGCCGGCATGATTCCCC-3'
Primer P16	5'-GCTCTAGATGCCGATGCTGGTGGAGC-3'
Primer P17	5'-CGAGCTCCTCGAGGAAGGCTTCGC-3'
Primer P18	5'-CAGGAGCGTGGCGGTAGCTCCCCCCAACCGG-3'
Primer P19	5'-CCGGTTGGGGGGAGCTACCGCCACGCTCCTG-3'
Primer P20	5'-GCTCTAGAGCATCCTGCTGATCGTCT-3'
Primer P21	5'-CCAAGCTTATGAGCCCGTCCGAAAACAT-3'
Primer P22	5'-CGGGATCCCTAGCGTTCGCCCTGGC-3'
Primer P23	5'-CAAGCTTATG GTAGCTATTACCCACACACC-3'
Primer P24	5'-CGGATCCTCAGCGGGTGCCGAAGAC-3'
Primer P25	5'-CGGATCCATGGTAGCTATTACCCACACACC-3'
Primer P26	5'-TTGCGGCCGCGCGGGTGCCGAAGAC-3'
Primer P27	5'-GCTCTAGAGAGTTTGCGGCCCCGCT-3'
Primer P28	5'-GCTGCAGGTTGACCGTGGCCTGTCCC-3'
Primer P29	5'-CCGTCCACGACAACCTACCTCGCTTGGAAG-3'
Primer P30	5'-CTTCCAAGCGAGGTAGGTTGTCGTGGACGG-3'
Primer P31	5'-TCCACGACAATGTGCCTCGCTTGGAAGCTCACGCTCCTCACACAGACGAAAAC-3'
Primer P32	5'-GTTTTCGTCTGTGTGAGGAGCGTGAGCTTCCAAGCGAGGCACATTGTCGTGGA-3'
Primer P33	5'-TCCACGACAACCCACCTCGCTTGGAAGCTCACGCTCCTCACACAGACGAAAAC-3'
Primer P34	5'-GTTTTCGTCTGTGTGAGGAGCGTGAGCTTCCAAGCGAGGTGGGTTGTCGTGGA-3'

Table S4. qRT-PCR primers used in this study, related to **Figure 1 to 6.**

Name	sequences	Name	sequences
Csy1 F	5'-CCGCAGAACATCAGTCAGTT-3'	gacA F	5'-CCGACTGCGGTGAAGACTGT-3'
Csy1 R	5'-ATGCTCGAAGACCGAAGAGT-3'	gacA R	5'-GGTGACTACCACGACCTTGATG-3'
Cas1 F	5'-GACATTTCTCCCAGCGAACT-3'	rsmY F	5'-GCCAAAGACAATACGGAAAC-3'
Cas1 R	5'-TGTTCCAGTAGTGCGAATGC-3'	rsmY R	5'-TCTATCCTGACATCCGTGCT-3'
Csy2 F	5'-AGTCGGAATCTCCCTCGATA-3'	bfmR F	5'-GCGAGCTGGTAGGCAACTA-3'
Csy2 R	5'-TCAGGTTGAAGACCTTGGTG-3'	bfmR R	5'-GATGTCGAGGACGATCAGG-3'
Csy3 F	5'-ATGTCCTGCTCGAAGTGGT-3'	lasR F	5'-CTTCATCGTCGGCAACTAC-3'
Csy3 R	5'-CTTGCTCTTCTGGCCTTTCT-3'	lasR F	5'-GTCTGGTAGATGGACGGTTC-3'
Cas3 F	5'-CGACAACTCGATGAACTGCT-3'	lasI F	5'-TGCGTGCTCAAGTGTTCAAGG-3'
Cas3 R	5'-GCGAGTACGACGAACAGATG-3'	lasI R	5'-TGTCCAGAGTTGATGGCGAAA-3'
Csy4 F	5'-CCGTACCGTCAGGTCAGTC-3'	rhlR F	5'-GCTCCTCGGAAATGGTGGT-3'
Csy4 R	5'-GAGCCTCCTCCTCACTCAGA-3'	rhlR R	5'-GGAAAGCACGCTGAGCAAAT-3'
16S F	5'-TGGTTTAATTCGAAGCAACG-3'	rhlI F	5'-TCCGCAAACCCGCTACATC-3'
16S R	5'-ATCTCACGACACGAGCTGAC-3'	rhlI R	5'-TCTCGCCCTTGACCTTCTGC-3'
exsA F	5'-GGTAAACAAGGAAGAGGGCGTAT-3'	rpoS F	5'-GCCTGAACGAACGGGTGACT-3'
exsA R	5'-GGACGAAGCCTTGTAGAAACTGG-3'	rpoS R	5'-CACCTCACGCTGCTTGTCG-3'
gacS F	5'-CAGCAGGACTACCTCACGAC-3'	bfmS F	5'-GACTACCTCAAGGAGCGCAT-3'
gacS R	5'-AGGTCGCGGAGATTGAAAGG-3'	bfmS R	5'-CTCTTCGAGATCGTTCCACA-3'
phzM F	5'-GCTACGCTAATACCCCCACC-3'	rpoA R	5'-TTAGCCAGGGTCAGCGTCA-3'
phzM R	5'-AGCTGTAGAAGTCTTCGCCG-3'	rpoA F	5'-TCGCATCCTGTTGTCCTCCA-3'
glpF F	5'-GGCGGTGATCATGGCTCTTA-3'	phes F	5'-TCAATATTCCGGGCCACCAC-3'
glpF R	5'-GGAAGTAGGGAATCTCGCGG-3'	phes R	5'-AATTCCTCGATGGTGCCCTT-3'
cysT F	5'-CGTGCTCAATGGCTTGATCG-3'	vfr F	5'-GGCGAGCTGGGATTGTTC-3'
cysT R	5'-ACTTCCTTGGGAATGTCGGC-3'	vfr F	5'-GGCTGCCGAGGGTGTAGA-3'

Table S5. Templates for in vitro transcription, related to **Figure 6**.

T7-glpF (T7 promoter is underlined)	TAATACGACTCACTATAGGATGACCACCGCCGCCCCGACCCCGTCCC TGTTCGGCCAATGCCTGGCCGAAT….TCGCGCGCCATCTGCCGAGCG CCGCGGCGCCCGCCGAAGCCGAGCCGGAGAAGGTTCGCGCTTCCTG A (gene ID: PA14_17980 in Pseudomonas Genome DB)
T7-CRISPR array 1 (T7 promoter is underlined)	TAATACGACTCACTATAGGGTTCACTGCCGTATAGGCAGCTAAGAAAA CCACCCGCTACCACCGGCAGCCGCACC…GACGCGTTCACTGCCGTATA GGCATAGGCAGCTAAAAAATGTCCCGAAGTTCATAAGCGGGCTTCGGG CGATTTCACTGCCACATAGGTCGTCAAGAAACGGCCAGCAGCCCTGAAG TATCGATTGATGCGGTTCGCTGTCGGCCGGGGTCACCAGTCGAAACGAA GTCCCTTTCCATGGGACTTCGTTGCGGACATGC
T7-CRISPR array 2 (T7 promoter is underlined)	TAATACGACTCACTATAGGGTTCACTGCCGTGTAGGCAGCTAAGAAA ATCAGCCGGACGTTGTAGTAGTCGAGCGCGGTGTTCACTGCCGTGTA GGCAGCTAAGAAAGCCGG…TAAGAAATTCACGGCGGGCTTGATGTC CGCGTCTACCTGGTTCACTGCCGTGTAGGCAGCTAAGAAATTGCCGA GTACGATGCCTGATACATGAATCCAGTTCACTGCCGTGTAGGCAGCT AAGAAACTCGAACCCACCTCGGCCACAACAGCCGCCGGGTTCGCTG CCGTCTAGGCAGAACCACCCTCCCCATCCCACTACCAAACATCCGAA TATAAAGTTCCTA
T7-crRNA$_{CR1\text{-}sp1}$-M1 (T7 promoter is underlined; blue is mutation in seed-region base-pairing site)	TAATACGACTCACTATAGGGTTCACTGCCGTATAGGCAGCTAAGAAA ACCACCCGCTACCACCGGCAGCCGCACCGGTTGTTCACTGCCGTATA GGCAGCTAAGAAA
T7-crRNA$_{CR1\text{-}sp1}$-M2 (T7 promoter is underlined; blue is mutation in seed-region base-pairing site)	TAATACGACTCACTATAGGGTTCACTGCCGTATAGGCAGCTAAGAAA ACCACCCGCTACCACCGGCAGCCGCACCAACCGTTCACTGCCGTATA GGCAGCTAAGAAA
T7-crRNA$_{CR1\text{-}sp1}$-M3 (T7 promoter is underlined; blue is mutation in seed-region base-pairing site)	TAATACGACTCACTATAGGGTTCACTGCCGTATAGGCAGCTAAGAAA ACCACCCGCTACCACCGGCAGCCGCAAAGGCCGTTCACTGCCGTATA GGCAGCTAAGAAA
T7-crRNA$_{CR1\text{-}sp1}$-M4 (T7 promoter is underlined; blue is mutation in seed-region base-pairing site)	TAATACGACTCACTATAGGGTTCACTGCCGTATAGGCAGCTAAGAAA ACCACCCGCTACCACCGGCAGCCGGTCCGGCCGTTCACTGCCGTATA GGCAGCTAAGAAA
T7-crRNA$_{CR1\text{-}sp1}$-M5 (T7 promoter is underlined; blue is mutation in seed-region base-pairing site)	TAATACGACTCACTATAGGGTTCACTGCCGTATAGGCAGCTAAGAAA ACCACCCGCTACCACCGGCAGCATCACCGGCCGTTCACTGCCGTATA GGCAGCTAAGAAA
T7-crRNA$_{CR1\text{-}sp1}$-M6 (T7 promoter is underlined; blue is mutation in seed-region base-pairing site)	TAATACGACTCACTATAGGGTTCACTGCCGTATAGGCAGCTAAGAAA ACCACCCGCTACCACCGGCAATCGCACCGGCCGTTCACTGCCGTATA GGCAGCTAAGAAA

Transparent Methods

Bacterial strains and growth conditions.

Supplementary Table 2 lists all bacterial strains and phages used in this study, respectively. *P. aeruginosa* UCBPP-PA14 (PA14-WT), *P. aeruginosa* PAO1 WT and mutants were grown on lysogeny broth (LB) agar or liquid medium at 37 ℃. When required, LB was supplemented with ampicillin (50 μg/ml) and chloramphenicol (12.5 μg/ml) or tetracycline (10 μg/ml), or kanamycin (100 μg/ml) to maintain the plasmids.

Plasmid construction.

Targeted or "primed" plasmids by *P. aeruginosa* 14 type I-F CRISPR-Cas system were generated as follows. The chloramphenicol acetyltransferase (CAT) gene, under the pCAT promoter was amplified using primers P1 and P2 (Table S3) and ligated into the *Bam*HI and *Pst*I sites of pgRNA to generate untargeted plasmid. The oligonucleotides corresponding to type I-F protospacer CRISPR array 1 spacer 1 (primers P3-4) and CRISPR array 2 spacer 1 (primers P5-6) were synthesized and annealed. After that, these protospacers were ligated to untargeted plasmid digested with *Hind*III and *Bam*HI and transformed into strain *E. coli* DH5α, and positives clones (CR1-sp1 or CR2-sp1 plasmids) were used for next experiments. Primed plasmids were constructed by inserting a protospacer CRISPR array 2 spacer 1 [primers P7-8] containing a single base mutation of the seed regions in the protospacer regions and ligated to untargeted plasmid digested with *Hind*III and *Bam*HI. Using primers 9-12, we screened the positive plasmids.

Construction of mutant strains.

To obtain the gene-deficiency *P. aeruginosa* UCBPP-PA14 strain, gene deletion of PA14 was constructed using the suicide vector pCVD442. A 500 bp up and downstream of gene were amplified by using primers 13-16 (*CdpR*) or 17-20 (*vfr*) and cloned into the *Sac*I and *Xba*I sites of pCVD442 vector. The constructed plasmids were electroporated into PA14-WT or related-mutant strains using an Electroporator 2510 systems (setting: 25 μF, 200 Ω, 2.5 kV; Eppendorf, Hauppauge, NY) according to Li et al (Li et al., 2016) to get the deficiency mutant. For complementation, *CdpR* and *vfr* gene were amplified from PA14-WT genomic DNA using primers 21-22 and 23-24 by PCR and cloned into the *BamH*I and *Hind*III sites of pAK1900 vector that was electroporatored into the corresponding mutant strain. All enzymes used in the present study were from New England Biolabs (Ipswich, MA).

RNA isolation and qRT-PCR.

Total RNA was prepared from *P. aeruginosa* using TRIzol (Ambion, Waltham, MA). The High Capacity cDNA Reverse Transcription Kit (ThemoFisher Scientific, Waltham, MA) was used to prepare cDNA and quantified with the qPCR (Table S4) using Maxima SYBR Green qPCR Master Mix (ThermoFisher Scientific, Waltham, MA).

Plasmid retention assay.

PA14-WT, PA14-Δ*cdpR*, PA14-Δ*cdpR/p-cdpR* or PA14-ΔTCR strains were grown to OD_{600}=0.6 and washed three times with 300 mM sucrose and then were electroporated with PA14 type I-F CRISPR-Cas targeted plasmid CR1-sp1 or CR2-sp1 or untargeted plasmid. Colonies containing the plasmid CR1-sp1 or CR2-sp2 were cultured in LB and grown at 37 ℃ with shaking for 5 h in the presence or absence of 100 μM baicalein. Colony forming units (CFUs) were counted on LB agar with and without ampicillin (50 μg/mL) and chloramphenicol (12.5 μg/mL). The percentage of plasmid retention was calculated.

Transformation of efficiency assay.

PA14-WT, PA14-Δ*cdpR*, PA14-Δ*cdpR/p-cdpR*, PA14-ΔTCR, PA14-Δ*vfr*, PA14-Δ*vfr/p-vfr*, PA14-Δ*cdpR*/Δ*vfr*, PA14-Δ*cdpR*/Δ*vfr/p-vfr*, PA14-Δ*lasI*, PA14-Δ*rhlI*, PA14-Δ*lasI*/Δ*rhlI*, PA14-Δ*cdpR*/Δ*lasI*, PA14-Δ*cdpR*/Δ*rhlI*, or PA14-Δ*cdpR*/Δ*lasI*/Δ*rhlI* were electroporated with 1μg CR1-sp1 or CR2-sp1 plasmid and added 1 mL LB for shaking 1 h at 37 ℃. Next, they were plated on lysogeny broth medium containing ampicillin and chloramphenicol and incubated overnight. CFUs were quantified and the transformation of efficiency was calculated as the percentage colonies transformed by CR1-sp1 or CR2-sp1 compared with untargeted plasmid.

Adaptation assay.

"Primed" plasmids were electroporated into PA14-WT, PA14-Δ*cdpR*, PA14-Δ*cdpR/p-cdpR*, PA14-ΔTCR, PA14-Δ*vfr*, PA14-Δ*vfr/p-vfr*, PA14-Δ*cdpR*/Δ*vfr*, PA14-Δ*cdpR*/Δ*vfr/p-vfr*, PA14-Δ*lasI*, PA14-Δ*rhlI*, PA14-Δ*lasI*/Δ*rhlI*, PA14-Δ*cdpR*/Δ*lasI*, PA14-Δ*cdpR*/Δ*rhlI*, or PA14-Δ*cdpR*/Δ*lasI*/Δ*rhlI* mutant strains and cultured in LB medium containing ampicillin (50 μg/mL) and chloramphenicol (12.5 μg/mL) in the present or absent of 100 μM Baicalein at 37 ℃ overnight. CRISPR expansion for integration of new immunity spacers were determined by RT-PCR with DreamTaq Green PCR Master Mix (ThermoFisher Scientific) using primer primers P9-10 for CRISPR array 1 and primers P11-12 for CRISPR array 2. PCR products were separated by 1.5% agarose gel electrophoresis with staining with ethidium bromide, and band intensities were quantified using ImageJ (Schneider et al., 2012).

Phage isolation and plaque assay.

Phages used in the present work listed in Supplementary Table 1 were isolated from lysogen in LB culture with growing for 2 days at 37 ℃. The lysate was centrifuged at 10,000g for 10 min and removed the supernatant to a fresh tube. After that adding a few drops of chloroform to store at 4 ℃. These phage lysates were subjected to plaque assay on bacterial lawns of PA14-WT, PA14-Δ*cdpR*, PA14-Δ*cdpR/p-cdpR* or PA14-ΔTCR strains. Plaque assay were conducted at 37 ℃ on LB agar (1.5%) plates with a lower percentage of LBTop agar (0.8%). $1X10^8$ bacteria cells with or without 100 μM baicalein were mixed with 4 mL LBTop agar and poured onto LB agar plate as an even layer. Allow top agar to cool for 30 min, onto which spot 3.5

μL of each phage lysate on the lawn and incubated overnight. The observed circular zones of clearing that lyse of the tester strains. The adaptation Assays were according to Heler et al (Heler et al., 2015).

Expression and purification of the Vfr protein.

The full-length *vfr* gene (primers 25-26) was cloned into pET-28a with *BamHI* and *NotI* and transformed into *E. coli* BL21 strain to induce Vfr expression by adding isopropyl-β D-thiogalactoside (IPTG) to 1 mM final concentration for 7 h at 25 °C. Purified recombinant Vfr protein was used by Ni-NTA column.

β-Galactosidase assay.

The *cas1* promoter (primers 27-28) or *cas1*-Δ promoter (primers 27-30) were cloned into an integrative *lacZ* reporter plasmid pVIK107-Tc. The integrative vectors were introduced into various PA14-WT or mutants for β-galactosidase assay according to Joshua P. Ramsay (Ramsay, 2013). Briefly, all integrative *lacZ* reporter strains were electroporated and grown in LB with tetracycline at 30 ℃. OD_{600} of the strains was recorded for normalization. The 10 μl each sample was added to the 100 μl reaction buffer (PBS, 2 mg/ml lysozyme, 250 μg/ml 4-Methylumbelliferyl-D-galactoside). The relative fluorescence intensity was monitored using Bio TeK Synergy HT Multi-Mode Microplate Reader (Bio-Tek) with excitation 365 nm, emission 455 nm at 37 ℃ for interval 1 min over 30 min. The plate-reader software calculated V_{max} automatically that was normalized to the OD_{600} of the sample (RFU/s/ OD_{600}).

Electrophoretic mobility shift assays (EMSA).

Different concentrations of the recombinant Vfr were incubated with the *cas1* promoter (primers 29-30) or *cas1*-Δ promoter (primers 26-30) PCR products and Vfr CRE (primers 31-32) or CRE-Δ (primers 33-34) probes in 20 μl binding reaction and incubated 20 min at room temperature according to the EMSA Kit (ThermoFisher Scientific). At the end of inubation period, adding EMSA gel-loading solution to the samples that were analyzed by 5% or 15% polyacrylamide gel electrophoresis in 0.5X TBE buffer (ThermoFisher Scientific) at 80 V for 90 min. The gels were stained by the SYBR Green EMSA Nucleic Acid Gel Stain and visualized using Bio-Rad Gel Doc XR+.

Co-immunoprecipitation (Co-IP) combined with northern blot.

PA14-WT, PA14-Δ*cdpR*, PA14-Δ*cdpR/p-cdpR* strains containing pMQ70-cas3-6xHis or pMQ70-csy3-6xHis plasmid were cultured with Arabinose to OD_{600}=1.0 at 37 ℃. After three times washing by ice-cold 1xPBS, expose the strains to 80, 000 μJ/cm^2 of 254-nm UV irradiation using a Stratalinker 1800 UV cross-linker and immediately plate it on ice. Using the 0.1-mm diameter glass beads at a frequency of 30/s for 15 min to lysis samples with wash buffer (50 mM sodium phosphate, 300 mM NaCl, 0.1% IGEPAL, 10 mM imidazole, 0.2% protease inhibitor cocktail). The samples were incubated with well-mix protein A/G magnetic beads binding the anti-His antibody for 90 min. After five times washing by wash buffer, keep the samples in

the magnetic rack and then added 300 μl of proteinase K reaction mix (50 mM Tris-HCl PH7.8, 50 mM NaCl, 0.1% IGEPAL, 10 mM imidazole, 1% SDS, 5 mM EDTA, 5 mM ß-mercaptoethanol, 0,1 U/μl recombinant RNase inhibitor, 33 μg/μl) to the samples for 2 h at 55 °C with gentle agitation. Add 0.9 ml of TriReagent LS (zymo research) to RNA extraction according to the standard TriReagent LS protocol. Total RNA were run on a 6% TBE-urea polyacrylamide gel for northern blot as described (Cady and O'Toole, 2011).

In vitro cleavage assay

The *glpF*, *cysT*, and *phzM* RNA substrate and the crRNA of CRISPR array were generated by using the MEGAscript T7 kit according to manufacturer's protocols with TURBO DNase treatment. DNA templates for in vitro transcription were listed in the Table S5.

The *P. aeruginosa* Cas3 and Csy complex were expressed and purified as described in Li and MaryClare F. Rollins (Li et al., 2016; Rollins et al., 2017). All cleavage assays were performed as described in (Li et al., 2016).

Statistical analysis.

Statistical analysis was performed with GraphPad (GraphPad Software, LaJolla, CA) using One way ANOVA plus Tukey test. No significant difference between samples is indicated as $P>0.05$ and statistically significant differences are indicated as $*P<0.05$, $**P<0.01$.

Supplemental References

Cady, K.C., Bondy-Denomy, J., Heussler, G.E., Davidson, A.R., and O'Toole, G.A. (2012). The CRISPR/Cas adaptive immune system of Pseudomonas aeruginosa mediates resistance to naturally occurring and engineered phages. J Bacteriol *194*, 5728-5738.

Cady, K.C., and O'Toole, G.A. (2011). Non-identity-mediated CRISPR-bacteriophage interaction mediated via the Csy and Cas3 proteins. J Bacteriol *193*, 3433-3445.

Heler, R., Samai, P., Modell, J.W., Weiner, C., Goldberg, G.W., Bikard, D., and Marraffini, L.A. (2015). Cas9 specifies functional viral targets during CRISPR-Cas adaptation. Nature *519*, 199-202.

Høyland-Kroghsbo, N.M., Paczkowski, J., Mukherjee, S., Broniewski, J., Westra, E., Bondy-Denomy, J., and Bassler, B.L. (2017). Quorum sensing controls the Pseudomonas aeruginosa CRISPR-Cas adaptive immune system. Proc Natl Acad Sci U S A *114*, 131-135.

Jacobs, M.A., Alwood, A., Thaipisuttikul, I., Spencer, D., Haugen, E., Ernst, S., Will, O., Kaul, R., Raymond, C., and Levy, R. (2003). Comprehensive transposon mutant library of Pseudomonas aeruginosa. Proc Natl Acad Sci U S A *100*, 14339-14344.

Li, R., Fang, L., Tan, S., Yu, M., Li, X., He, S., Wei, Y., Li, G., Jiang, J., and Wu, M. (2016). Type I CRISPR-Cas targets endogenous genes and regulates virulence to evade mammalian host immunity. Cell Res *26*, 1273-1287.

Patterson, A.G., Jackson, S.A., Taylor, C., Evans, G.B., Salmond, G.P., Przybilski, R., Staals, R.H., and Fineran, P.C. (2016). Quorum sensing controls adaptive immunity through the regulation of multiple CRISPR-Cas systems. Mol Cell *64*, 1102-1108.

Ramsay, J. (2013). High-throughput ß-galactosidase and ß-glucuronidase Assays Using Fluorogenic Substrates. Bio-protocol *3*, e827-e827.

Rollins, M.F., Chowdhury, S., Carter, J., Golden, S.M., Wilkinson, R.A., Bondy-Denomy, J., Lander, G.C., and Wiedenheft, B. (2017). Cas1 and the Csy complex are opposing regulators of Cas2/3 nuclease activity. Proc Natl Acad Sci U S A *114*, E5113-E5121.

Schneider, C.A., Rasband, W.S., and Eliceiri, K.W. (2012). NIH Image to ImageJ: 25 years of image analysis. Nat methods *9*, 671-675.

Zegans, M.E., Wagner, J.C., Cady, K.C., Murphy, D.M., Hammond, J.H., and O'Toole, G.A. (2009). Interaction between bacteriophage DMS3 and host CRISPR region inhibits group behaviors of Pseudomonas aeruginosa. J Bacteriol *191*, 210-219.